U.PORTO
FEUP FACULDADE DE ENGENHARIA
UNIVERSIDADE DO PORTO
INSTITUTO DE CIÊNCIAS BIOMÉDICAS ABEL SALAZAR
UNIVERSIDADE DO PORTO

The role of hypoxia mediators in inflammatory cells during asthma in mice

Ana Meneses

MSc Thesis

Integrated Masters on Bioengineering
Molecular Biotechnology

Supervisor: Prof. Dr. Ben Wielockx
Co-supervisor: Prof. Dr. Manuel Vilanova

June 2015

The role of hypoxia mediators in inflammatory cells during asthma in mice

Ana Meneses

MSc Thesis

Integrated Masters on Bioengineering
Molecular Biotechnology

Project Supervisor: Prof. Dr. Ben Wielockx
Technische Universität Dresden– Medizinisch Theoretisches Zentrum
Department of Pathobiochemistry

Project Co-Supervisor: Prof. Dr. Manuel Vilanova
Universidade do Porto – Instituto de Ciências Biomédicas Abel Salazar

“Life should not be a journey to the grave with the intention of arriving safely in a pretty and well preserved body, but rather to skid in broadside in a cloud of smoke, thoroughly used up, totally worn out, and loudly proclaiming "Wow! What a Ride!” ” – Hunter S. Thompson

Abstract

Asthma is a complex disease characterized by the interaction of several different cell types with chronic tissue remodeling that leads to the observed symptoms of reversible airflow obstruction and airway hyper-responsiveness (AHR).

Although several advances have been made in the characterization of this disease, no viable treatment has been created so far. Since the activation of the hypoxia response pathway during the asthmatic response aggravates the outcome of this disease, the manipulation of this pathway emerges as an attractive candidate for novel therapy development.

The cell type specific role of the hypoxia-inducible factor (HIF) pathway during the asthmatic response is yet to be described. This work was therefore conducted with the purpose of investigating the role of the oxygen sensors prolyl hydroxylase domains (PHDs) in the T cell compartment as well as in the myeloid compartment during allergic asthma in mice. Ovalbumin (OVA) and house dust mite (HDM) were used as antigens to induce the asthmatic phenotype.

PHD2 was found to have a protective role in the T cells during asthma, as mucus secretion and vascular remodeling were observed to be increased upon deletion of this protein.

Although deletion of PHD2 in the myeloid compartment did not seem to affect asthma development, combined deletion with PHD3 resulted in higher cell infiltration in the bronchoalveolar lavage fluid (BALF) upon asthma, with a marked influx of $CD4^+$ T cells and eosinophils.

This work has thus described for the first time a protective role of PHD2 in the T cells during asthma, indicating also a possible compensatory role of PHD3 in the myeloid compartment in the control of this disease. Further research is required in the characterization of the role of these proteins in the immune cells involved in the asthmatic outcome, hopefully leading to new ways to attenuate the symptoms of this disease.

Acknowledgements

I would like to express my sincere gratitude to all of those that supported me throughout my Master, particularly during the work that now culminates in my Master thesis.

First and foremost, I want to thank Professor Ben Wielockx, for accepting me in your group and allowing me to develop this project that grew on me and made me grow as a research scientist. I appreciate all of the patience, support and encouragement, as well as all of the discussions that allowed this work to take a step further. Thank you for believing that I could do this and letting me learn from my mistakes. I hope can learn more from you in the future!

I would also like to express my gratitude to Professor Triantafyllos Chavakis, head of the department of Pathobiochemistry, for granting me the possibility of performing this work in his department and assuring the financial aid during this period of my stay, which was essential for me to complete this work.

I want to express my recognition to Dr. Kristin Franke, who supervised me in the initial period of my stay and who taught me everything that allowed me to be in the place I am now. Thank you for making every stressful moment in the lab seem like nothing.

I also want to express my gratitude to Dr. Rashim Pal Singh, who, since Kristin left, has helped me gain my independence in the lab. Thank you for the patience, the fruitful discussions and the knowledge you've transmitted to me.

I want to take this opportunity to thank Prof. Manuel Vilanova, for accepting the co-supervision of this thesis and Prof. Luis Vieira, without whose determination I wouldn't be here finishing it.

To my "lovely assistants", thank you very much for all of the help you've given me during those long experiment days. I truly don't know how I would manage without you by my side and I hope you know I will be there when you need too! Working with you has been one of the best experiences I've had, thank you for creating a great lab environment.

To my family, especially my mom, dad and brother, for always believing in me and cheering me up when I didn't. Thank you for being there even when I am difficult to understand and allowing me this opportunity to study abroad and, most of all, pursuit my dreams. Wherever I go, you'll always come with me.

To my Dresden family, you are great. Seriously, thank you for giving me a home in a country that is not mine (and making it feel like it actually is)! I really appreciate all of the fun moments, the stupid and deep conversations and all of your worries, I'm happy to have met each and every single one of you and I'm glad we'll have more adventures together in the future.

To the friends that stayed in Portugal but were always here with me when I needed: thank you for everything. It's been great growing with you and I truly hope all of your futures are bright, wherever that might be. It's been a hell of a ride!

Finally, to my travel companion, Isa, who has been through as much (and maybe even more) than I've been, but still listens to me complain every time. Thank you for easing the transition to this crazy country and for all the stories that will prevail. And of course, thank you for not killing me in the process. In my defense, you're difficult too and that's why I'm sure that even now we're going in separate ways, we'll still be there to annoy each other when needed!

Table of Contents

List of Figures and Tables

Abbreviations

ABTS	2,2’-Azino-bis(3-ethylbenzothiazoline-6-sulfonic acid)
AHR	airway hyper-responsiveness
Alum	aluminium hydroxide
AM	alveolar macrophage
APC	antigen-presenting cell
BALF	bronchoalveolar lavage fluid
BSA	bovine serum albumin
cKO	conditional knockout
COPD	chronic obstructive pulmonary disease
DAPI	4',6'diamidino-2-phenyldole
DC	dendritic cell
DHB	ethyl 3,4-dihydroxybenzoic acid
DP	double positive
ECL	electrochemiluminescence
ECP	eosinophil cationic protein
EDTA	ethylenediaminetetraacetic acid
EGFR	epidermal growth factor receptor
ELISA	enzyme-linked immunosorbent assay
EPO	eosinophil peroxidase
FCS	fetal bovine serum
FcεRI	high-affinity Fc receptor for IgE
FcεRII	low-affinity Fc receptor for IgE
FoxP3	forkhead box P3
GM-CSF	granulocyte-macrophage colony-stimulating factor
H&E	Haemotoxylin and Eosin
H_2SO_4	sulfuric acid
HCT	hematocrit
HDM	house dust mite
HGB	hemoglobin
HIF	hypoxia-inducible factor

HRE	hypoxic response element
HRP	horseradish peroxidase
IFN-γ	interferon-γ
Ig	immunoglobulin
IL	interleukin
IM	interstitial macrophage
IN	intranasal
IP	intraperitoneal
iTreg	induced Treg
LPS	lipopolysaccharide
LTC	leukotriene C
M1	classically activated macrophages
M2	alternatively activated macrophages
MBP	major basic protein
MFI	mean fluorescence intensity
MHC	major histocompatibility complex
MT	Masson Trichrome
nTreg	natural Treg
O.D.	optical density
OVA	ovalbumin
PAMP	pathogen-associated pattern
PAS	Periodic Acid Schiff
PBS	phosphate buffer saline
PFA	paraformaldehyde
PH	pulmonary hypertension
PHD	prolyl hydroxylase domain
PLT	platelet
PRR	pattern-recognition receptor
RA	retinoic acid
RBC	red blood cells
RORγt	retinoic acid receptor-related orphan receptor-γt
Siglec-F	sialic acid-binding immunoglobulin-like lectin F
siRNA	specific small interfering RNA
SMC	smooth muscle cell
T-bet	T-box transcription factor

TCR	T-cell receptor
TGF-β	transforming growth factor β
Th	T helper
Th17	(IL-17)-producing T helper
TLR	toll-like receptor
TNF-α	tumor necrosis factor α
Treg	regulatory T cell
VEGF	vascular endothelial growth factor
VHL	Von Hippel–Lindau protein
WBC	white blood cell
WT	wild type

Introduction

Asthma is a chronic inflammatory disease that affects more than 300 million people, leading to the death of approximately 25.000 people per year worldwide[1]. The prevalence of this disease has been increasing globally during the second half of the 20th century, especially in economically developed countries, making it the most common chronic lung disease worldwide[2,3]. This increase has been associated to environmental aspects such as air pollution, eating and hygienic habits and drugs, but no single cause has been identified[4].

Asthmatic individuals tend to be more susceptible to these stimuli due to pre-existing atopy, a predisposition to developing certain allergic hypersensitivity reactions[5]. Other risk factors involve specific genetic variations in the regulators of type 2 inflammation, but there are also less understood vulnerabilities that could be associated with the increase of asthmatic cases[5].

The first symptoms of asthma usually appear during childhood, when the patients have mild to sporadic episodes of airway obstruction[3]. These are triggered in vulnerable individuals by exposure to virus or airborne pollutants that lead to the activation of the epithelium[5]. The aberrant immune responses to stimuli are established when the immune system is still plastic, which may lead to persistent changes in cell behavior and, consequently, asthma endurance throughout the whole life[5].

Asthma can also be developed later in life, being the age of onset a crucial factor in disease phenotype and development[3]. Early-onset asthma is associated with a more allergic phenotype, whereas late-onset asthma is associated with high eosinophil infiltration and inflammation and, generally, fewer allergies[3]. These patients reveal more severe airflow obstruction and are more prone to exacerbations[4].

Asthma is generally characterized as a T helper (Th)2-mediated condition[3]. This disease involves the activation of an array of inflammatory cells affecting the lower airways. Besides the T cells, the major mediators of the allergic response observed in asthma are the dendritic cells (DCs), eosinophils and mast cells[2], approached in more detail below.

The interaction of the aforementioned cells induces the symptoms of asthma, which can range from mild wheezing and cough to severe respiratory distress and even respiratory failure[6].

During the allergic inflammation that occurs in asthma, a hypoxic environment is created. Cells respond to this shortage of O_2 through the activation of the hypoxia response pathway, which perpetuates the highly pro-inflammatory response and consequent aggravation of the disease outcome[7,8].

Although the importance of this hypoxic environment in asthma is widely accepted[7], the role of the hypoxia response pathways' activation in the different immune cells involved in asthma is yet to be described. As myeloid and $CD4^+$ T cells play an important role in the pathogenesis of this disease, particularly the Th2 subset; the influence of this pathway in these cells' behavior represents a major cornerstone in the comprehension of this disease.

Modulators of the hypoxic response are being considered as possible therapies for diseases such as cancer[9], as in this disease the activity of this pathway is also augmented[10]. Further knowledge regarding the role of the hypoxia response mediators in the inflammatory cells of asthma may enable the generation of therapies based on similar principles.

1. Hypoxia

Animals have developed mechanisms that allow them to cope with hypoxia, a shortage in the oxygen level[11]. These allow the body to detect, adjust and react to different oxygen concentrations and are finely tuned at organ, tissue and cellular levels[12].

The transcriptional response to hypoxia is mediated by the HIF family. The proteins that constitute this family are heterodimeric, containing an α and a β subunit[11]. HIF1α, HIF2α and HIF3α are similar in structure and function. HIF1α is expressed in the majority of cell populations, as is HIF1β; whereas HIF2α/3α and HIF2β/3a are only expressed in a limited variety of tissues[8]. The regulatory complex is comprised of one of the -α subunits bound to HIFβ. The β subunits are constitutively expressed, being the HIF proteins regulated by post-transcriptional modifications on their -α subunits[11] (Figure 1).

Regulation of the HIF activity is mediated by a class of enzymes known as PHDs. Under normoxic conditions, the PHDs hydroxylate HIFα in specific proline domains, allowing its recognition and subsequent ubiquitination by the Von Hippel–Lindau protein (VHL). This leads to the proteasomal degradation of the HIFα subunit and, consequently, inactivation of the HIF protein[13,14].

As PHDs require O_2, iron, ascorbate and 2-oxoglutarate to exert their functions[15], under hypoxic conditions they are rendered non-functional and HIFα is stabilized, translocates

to the nucleus and binds to the HIFβ subunit. The formed heterodimer binds to hypoxic response element (HRE)-containing promoter regions, inducing the transcription of genes involved in cellular functions such as cell survival and proliferation, apoptosis, glucose metabolism and angiogenesis[11,14,16].

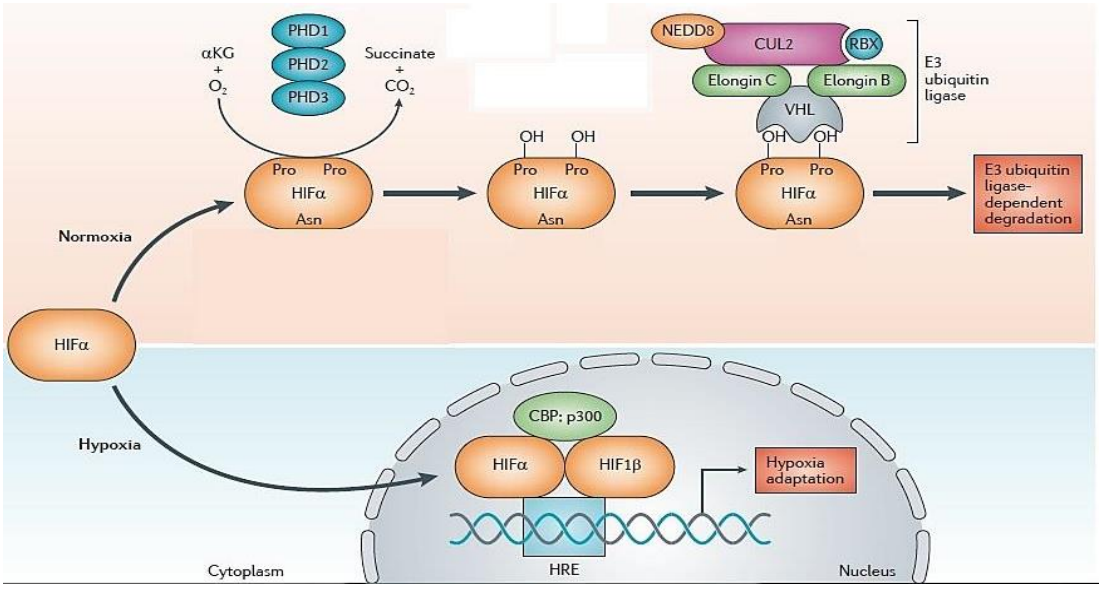

Figure 1 Molecular mechanism of the hypoxia response pathway. Adapted from Eltzschig et al, 2014.[9]

Three PHD isoforms have been described - PHD1, PHD2 and PHD3 - and all are capable of hydroxylating HIFα.[12, 15] However, PHD2 appears to be the major regulator of the hypoxic response[17], as elimination of this protein *in vitro* is sufficient to induce HIFα and systemic deletion in genetically engineered mice leads to embryonic lethality, an outcome not observed for embryos lacking either PHD1 or PHD3[18]. Expression of each PHD family member is distributed in distinct tissues, suggesting that these isoforms have distinct functions. In fact, each isoform has a different affinity for the inhibition of particular HIFα subunits; PHD2 has a stronger substrate preference for HIF1α, whereas PHD3 degrades preferentially HIF2α under hypoxia[12].

PHD3 is itself a target of HIF1α and its induction under hypoxic conditions leads to the negative regulation of HIF2α[15]. This feedback mechanism suppresses HIF activation under continued hypoxia[19], maintaining a tight balance between the activation of the aforementioned transcription factors[20].

The complex network of regulation of the hypoxic response plays a crucial role in several physiological as well as pathological processes. Therefore, the differential inhibition of PHDs has the potential to alter the characteristics of HIF activation in a selective manner and thus modulate these responses.

1.1. Hypoxia in Asthma

Inflammation and limited oxygen accessibility are hallmarks of asthma and other immunological responses to tissue damage[16].

Bronchial biopsies of asthmatic patients reveal increased activation of the hypoxia response pathway[8]. The activation of the HIF1α subunit has a pro-inflammatory connotation and leads to the activation of genes such as vascular endothelial growth factor (VEGF), which are implicated in airway remodeling. This pathway has also been associated with increased collagen synthesis and fibrosis[7].

Several studies have found increased levels of both HIF1α and PHD2 in animal models of asthma[7,8]. Using the PHD2 inhibitor ethyl 3,4-dihydroxybenzoic acid (DHB), an oxoglutarate analogue, Ahmad *et al.* observed a DHB dose-dependent increase of AHR in a mouse model of asthma, associated with an increased cell infiltration, mucus production and collagen deposition in the basal membrane of the epithelium[7].

Using a non-specific HIF inhibitor, Huerta-Yepez *et al.* have reported that the inhibition of this pathway reduced the allergic inflammation and lung remodeling in an OVA-triggered mouse model[21]. This group was also able to demonstrate that exposure to allergen in asthmatic patients leads to upregulated expression of HIF1α and VEGF[8]. To support these findings, recent work described that the systemic silencing of PHD2, the most important oxygen sensor, leads to the exacerbation of the asthmatic response[7].

However, the role of the hypoxia-inducible pathway in particular immune cells involved in the pathogenesis of the disease is yet to be fully understood. Toussaint et *al.* described a protective role of HIF1α through the immunoregulation of the asthmatic response by the macrophages in the lung[22]. Their work showed a positive regulation of HIF1α in the production of interleukin (IL)-10 by the interstitial macrophages (IMs) in the lung, with consequent inhibition of DC activation. This apparent contradictory result demonstrates the importance of the cell-specific modulation of the hypoxic response in the outcome of the disease. As inhibitors of PHD2 are being considered as drugs for several conditions, the role of this protein in asthmatic disease needs to be further analyzed[9].

2. Asthma Pathophysiology

Asthma is characterized by several alterations in the airways including exacerbated mucus production, shedding of epithelial cells, thickening of the bronchial walls, artery remodeling and proliferation and smooth muscle hyperplasia[2,3]. These changes lead to reversible airflow obstruction (dyspnea), AHR and sputum production[6].

Since 2008, the biological heterogeneity of asthma has been approached considering endotypes of this disease; disease subtypes with different functional mechanisms[5]. Until now, only one endotype has been described, based on the level of type 2 inflammation[5].

Type 2 inflammation is mainly regulated by Th2 cells and characterized by high antibody production and eosinophil infiltration[5,6]. Th2-high asthma patients represent the majority of asthmatic individuals and show higher levels of type 2 inflammation in the lung than healthy subjects, with high levels of IL-13 and eosinophilia[3,23]. Contrarily, Th2-low asthmatics possess eosinophil levels comparable to the normal healthy reference and are modeled by mechanisms yet to be understood[5]. The individuals that constitute this endotype might derive from a variety of endotypes with distinct characteristics that may include airway smooth muscle abnormalities, neutrophil infiltration or oxidative stress effects[23].

Nevertheless, both endotypes reveal the same physiological hallmarks of asthma[5]. These pathophysiological changes result in a lower lung capacity[6] and in the more severe spectrum of asthma the symptoms start overlapping with conditions such as chronic obstructive pulmonary disease (COPD)[3], leading ultimately to the death of the patient.

3. Asthmatic Immune Response

Asthmatic individuals show a hypersensitivity to airborne allergens triggered by immunoglobulin (Ig) E production, with activation of the airway epithelial cells, infiltration of immune cells in the lung tissue and remodeling of the epithelium and involving matrix[5].

The clinical phenotype of asthma is very heterogeneous, as the immune response involves several cell types. The classical view of this disease consists of a coordinated interaction between DCs and $CD4^+$ helper T lymphocytes, leading to the infiltration and activation of eosinophils and mast cells[2,3] (Figure 2).

Although this disease is characterized as a Th2-mediated condition, other innate/adaptive pathways are also involved[23].

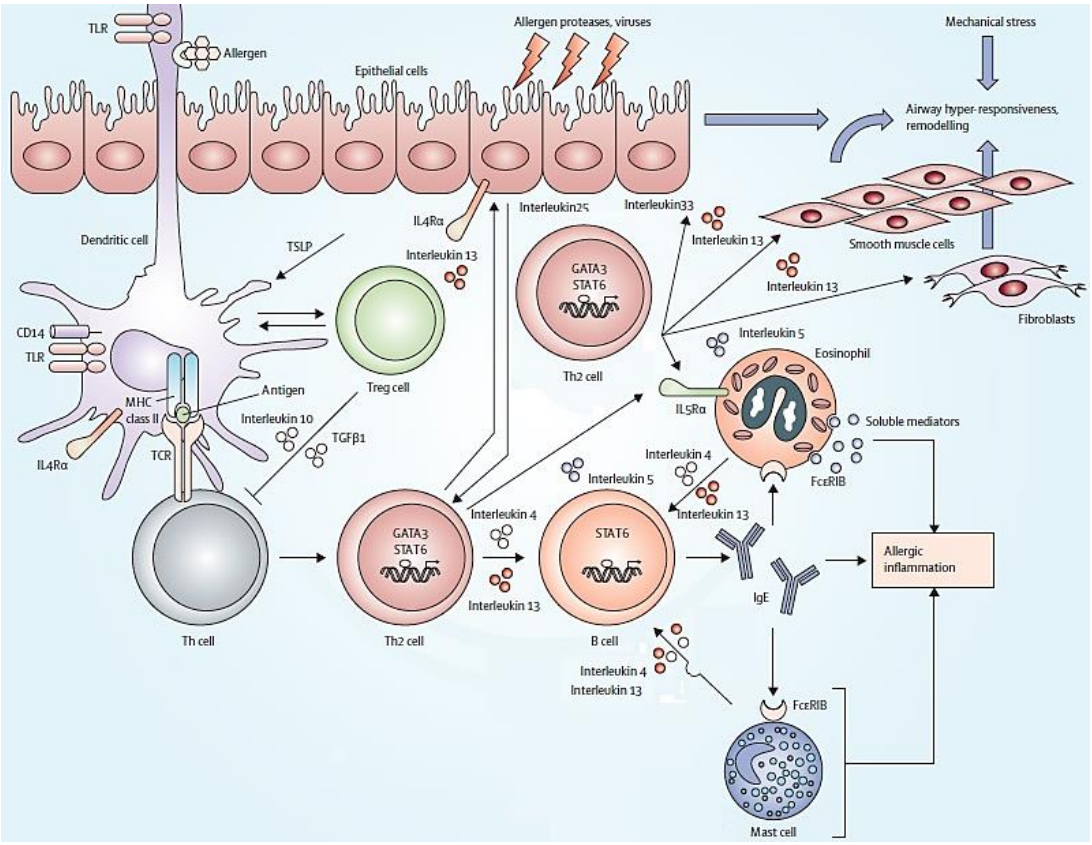

Figure 2 Principal immune pathways involved in the pathogenesis of asthma. The interactions between DCs, T cells, eosinophils and mast cells are depicted in the picture, as well as the resulting airway alterations. Adapted from Martinez et al, 2013.[3]

3.1. Sensitization

The airway epithelium serves as a barrier to airborne antigens, such as allergens, virus and pollutants. This structure is patrolled by immature DCs, which are distributed throughout the epithelial basement membrane of the lung, controlling the immune response to inhaled antigens[24].

In an asthmatic individual the tight junctions between epithelial cells are loosened, leading to the crossing of this barrier of antigens that wouldn't be harmful for healthy individuals but trigger the asthmatic response in susceptible people[6]. Under these conditions, the epithelial cells secrete a variety of mediators such as IL-25 and IL-33[3] that act as Th2-instructing signals for the lung DCs[24]. These regulators induce the augmented production of type 2 cytokines that prompt the ensuing events observed in asthma[5].

The lung DCs are in this way activated by the airborne antigen through the pattern-recognition receptors (PRR) on its surface. These cells maturate as they are at the same time stimulated by the cytokines produced by the epithelial cells[6,24]. Therefore, presentation of these antigens by the mature DCs leads to Th cells activation and maturation in the lymph nodes[6].

3.2. CD4+ T cell Activation

$CD4^+$ T cells are crucial regulators of the immune response and inflammatory diseases. Th cells are activated by DCs presenting processed cognate antigens, which induces their subsequent expansion[25].

During this induction, Th cells differentiate into either T helper type 1 (Th1), Th2, (IL-17)-producing T helper (Th17) and T regulatory (Treg) subsets under the control of lineage-specifying genes[3]. Whereas the first is restricted by the Th2 cytokines, Th17 cells can be present in considerable amounts in the asthmatic lung, regulating neutrophilic inflammation in Th2-low asthmatics. The contribution of these cells in human asthma, however, is not yet completely understood[6].

Th2 cells differentiate under the regulation of the transcription factor GATA3 and have a described role in humoral immunity[5]. After activation in the lymph nodes, these cells either migrate to the B-cell follicle to induce Ig class switching from IgM to IgE or travel back to the airway mucosa where they secrete pro-allergic cytokines such as IL-4, IL-5 and IL-13[6]. These cytokines, particularly IL-13, have a critical role in driving the key pathological features of this disease[2,6].

IL-4 promotes the Ig class switching, upregulation of adhesion molecules in the endothelium and eotaxin production. Besides its role in allergic sensitization, this cytokine also has a role in the AHR development and Goblet cell metaplasia[6]. Furthermore, IL-4 stimulates the differentiation of Th cells into a Th2 subset[5], resulting in a positive feedback loop.

Th2 cells are also important sources of IL-5 and granulocyte-macrophage colony-stimulating factor (GM-CSF), both having a role in eosinophil chemotaxis, maturation, survival and activation. Therefore, numbers of activated Th2 cells correlate with the number of eosinophils in the BALF[25].

IL-13 is extremely important in the induction and maintenance of AHR, tissue remodeling and Goblet cell metaplasia[6]. This cytokine mediates its effects directly on the airway epithelial cells through the IL-4Rα at the surface of these cells[4].

Therefore, the chronic activation of this Th cell subset is sufficient for the induction of inflammation and the remodeling observed in the asthmatic lung.

Th1 cells express the T-box transcription factor (T-bet) and secrete IL-2, interferon-γ (IFN-γ) and lymphotoxin-α; stimulating type 1 immunity, which is characterized by the elevated phagocytic activity[5].

In the T cells from the asthmatic airways the levels of T-bet mRNA are nearly undetectable. However, Th1 cells have been identified in the airway of some asthmatic patients, showing a possible role for these cells in this disease[4]. Th1 cells seem to participate in delayed-type hypersensivity reactions as this subset inhibits IgE synthesis through the secretion of IFN-γ[25].

Th17 cells express IL-17A and IL-17F and the transcription factors retinoic acid receptor-related orphan receptor-γt (RORγt) and RORα[26]. This subset appears to play a crucial role in neutrophilic inflammation and autoimmunity. The activation of these cells and subsequent IL-17 production also contributes to acute AHR, exacerbating the Th2 cell-mediated eosinophilic inflammation[26,27]. However, as IL-17 is also produced by other cell types such as mast cells, the particular role of this T cell subset still needs to be further studied[26].

Treg cells express the transcription factor forkhead box P3 (Foxp3) and are generated under the control of mucosal DCs with low expression of the major histocompatibility complex (MHC) class II and costimulatory molecules[4,28]. Most Tregs are generated during the thymic negative selection as a mechanism of self-tolerance development. Natural Tregs (nTregs) originate after strong T-receptor signaling upon self-antigen presentation by the DCs in the thymus during negative selection. This signaling is stronger than the one inducing conventional $CD4^+$ T cell commitment, but not enough to induce deletion, and therefore these cells do not go into apoptotic death[28].

As tolerance to nonpathogenic foreign antigens is also needed for the healthy function of the body, Treg cells can also be induced peripherally. Induced Tregs (iTregs) originate when mature, naïve $CD4^+$ T cells encounter antigens in peripheral lymphoid organs[29]. IL-2, transforming growth factor β (TGF-β) and retinoic acid (RA), produced by CD103-expressing DCs[28,29,30], are crucial factors for the induction of FoxP3 expression in these $CD4^+$ T cells.

Both nTregs and iTregs contribute to the inhibition of the inflammatory response that occurs upon asthmatic triggering, being the reduced or altered function of Treg cells a plausible explanation for the inappropriate immune response that occurs in this disease. Tregs

have been shown to control the Th2 responses[3] and exert their action via direct and indirect mechanisms, such as the production of anti-inflammatory cytokines, as IL-10 and TGF-β[29], expression of inhibitory molecules[26] and downregulation of MHC class II in the DCs surface[4].

3.3. B cell Activation and IgE Production

Under steady state conditions, IgE exists in insignificant levels in the circulation[31]. However, during asthma Th2 activated cells induce the isotype switching of B cells, leading to Ig class switching to IgE, with production of this antibody in high concentrations[6]. This induction is mediated by the IL-4 and IL-13 secreted by the Th2 cells[31], as well as physical interaction between the T and B cells through the CD40/CD40L molecules[32].

IgE interacts with the high-affinity (FcεRI) and low-affinity (FcεRII) Fc receptor for IgE at the surface of effector cells. While FcεRI is expressed only in mast cells, FcεRII is present at the surface of macrophages, DCs and eosinophils[31].

Through these receptors, IgE mediates several outcomes of the disease. This antibody stimulates the antigen presentation by the DCs to the Th cells in the lymph nodes when bound to their FcεRII[33], being also involved in the stimulation of pro-inflammatory cytokine production by the alveolar macrophages (AMs) when interacting with these cells[34]. IgE also has long-lived interactions with eosinophils, inducing their production of leukotrienes and thus contributing for the bronchoconstriction observed in the patients[23].

3.4. Macrophage Activation

Lung macrophages are comprised of cell populations with distinct characteristics divided according to their anatomic distribution into AMs and IMs. While the first are distributed along the alveolar space, representing the major immune population in the airway lumen under steady state conditions, the second are distributed along the interstitial space of the lung[35].

AMs represent the first line of defense against allergens and contribute to homeostasis through phagocytosis and inhibition of antigen presentation by the DCs with consequent inhibition of T cell activation. These cells are able to produce pro- and anti-inflammatory mediators, as well as IL-12 or IL-10 and IL-13, orienting the immune response triggered in the lung[36].

IMs, in turn, have the capacity to inhibit DC maturation and migration to the lymph nodes through the production of IL-10, preventing sensitization to airborne antigen. These

cells are less abundant than the AMs and have a lower phagocytic capacity comparing to these, but have higher antigen-presenting ability[34].

Under asthmatic triggering, however, both macrophage populations are activated by the IL-33 released by the damaged epithelium, differentiating into either classically (M1) or alternatively (M2) activated macrophages[34]. Whereas the first are induced upon stimulation of their toll-like receptors (TLR) by lipopolysaccharide (LPS) and produce relatively high amounts of pro-inflammatory cytokines such as IL-1β, IL-6 and tumor necrosis factor α (TNF-α); the latter differentiate under the stimulus of Th2 cytokines such as IL-4 and IL-13, producing IL-13, as well as anti-inflammatory cytokines such as IL-10 and TGF-β[37].

Both subsets have detrimental effects in the outcome of the disease. Although M2 macrophages produce IL-10, a pro-inflammatory cytokine, the production of TGF-β not only contributes for the regulation of the asthmatic response, but in high concentrations, induces fibrosis in the tissue[36,37]. The pro-inflammatory cytokines produced by M1 cells modulate the constriction of the smooth muscle cells (SMC) and activate eosinophils and fibroblasts, leading to the observed AHR and consequent airflow limitation[11,12,21,37].

Although under steady state conditions these cells inhibit the triggering of an allergic response, during asthma the inhibitory function of the macrophages in the tissue seems to be reduced, giving way to an inflammatory role of these cells in the disease.

3.5. Eosinophil Recruitment and Function

Eosinophils are important effector cells in the asthmatic response, comprising a large fraction of the cells in the airway lumen during this disease[38]. These granulocytes are also increased in circulation in asthmatic subjects, correlating with symptom scores[25,38].

Eosinophils migrate to the lung in response to the local production of IL-5 and eotaxin by the Th2 cells in this tissue. The first is specific for the eosinophils[25] and is the main pathogenic factor mediating the development of this granulocyte[39,40]. These cells release pre-formed mediators like leukotriene C4 (LTC)4, eotaxin, eosinophil cationic protein (ECP), major basic protein (MBP) and eosinophil peroxidase (EPO), as well as cytokines such as IL-4 and IL-13[39].

LTC4 leads to increased vascular permeability and is a strong smooth muscle constrictor, representing one of the major targets in asthma therapy[25]. While ECP induces mast cell degranulation and stimulates the mucus secretion in the airway, MBP not only activates mast cells but also directly alters smooth muscle contraction contributing to the development of AHR[39]. This basic protein is toxic for the pulmonary epithelial cells, damaging

the epithelium and contributing to its stress signaling[25]. EPO catalyzes the formation of highly reactive oxygen species, promoting oxidative stress and cell death by apoptosis[39].

Eosinophils promote the activation and proliferation of antigen-specific memory T cells and Th2 polarization through IL-4 production[41], being able to activate both naïve and primed T cells[39].

3.6. Mast cell Activation

Mast cells are key effectors in allergic disorders such as asthma. These cells are activated by cross-linking to IgE bound to the antigen through their FcεRI[2]. When activated, mast cells degranulate[4], secreting preformed inflammatory mediators, such as proteases, nucleotides, serotonin and histamine[42]. These factors induce vasodilation, formation of edema and bronchoconstriction[2,41].

These cells also produce IL-4, IL-13 and IL-25, which promotes the Th2-induced outcome, contributing to the perpetuation of the Th2 activation[4,42]. As many other effector cells, like Th2 cells, conduce to the same features of the disease, the relative influence of the mast cells to these symptoms remains to be thoroughly explored[41].

3.7. Neutrophil Recruitment

Some asthmatic individuals show marked neutrophilic inflammation. Neutrophil recruitment in these patients occurs through the IL-8 release from the bronchial epithelial cells, a cytokine that also prolongs neutrophil survival[43]. IL-8 production by the epithelial cells is stimulated through the IL-17A released by Th17 cells and mast cells[27,43].

These polymorphonuclear cells produce myeloperoxidase and elastase[43], which presence in the BALF correlates with the degree of bronchial AHR[27]. Other cytokine produced by these cells is oncostatin M that triggers the proliferation of SMC and fibroblasts, promoting airway remodeling[43].

It is unclear whether high neutrophil infiltration reflects a different asthma endotype or a different stage of severity[41].

4. Tissue Remodeling

4.1. Airway Remodeling

The continued stimulation of the epithelial, SMCs and fibroblastic cells by the cytokines produced by the inflammatory cells leads to AHR and remodeling[3].

The airway epithelium usually presents shedding of the ciliated cells, with metaplasia and hyperplasia of the Goblet cells, which produce mucus[6]. The high rates of proliferation of these cells lead to the increase of thickness of the airway wall from 10% to 300% of normal[4], prompting the decrease of the airway luminal diameter. This decrease is manifested in the bronchoconstriction observed in the patient.

The inflammation that occurs in asthma is not enough to lead to the chronic remodeling of the lung. However, this damages the epithelium, locking the epithelial cells in a repair phenotype, with an increase of the epidermal growth factor receptor (EGFR)[6]. Epithelial cells in this phase produce pro-fibrotic mediators, such as TGF-β and fibroblast growth factor, inducing epithelium-mesenchymal interactions[3,6]. These interactions induce the differentiation of fibroblasts surrounding the epithelium into myofibroblasts, which are involved in collagen deposition, leading to the increase of the thickness of the basement membrane[6].

Airflow limitation occurs as an outcome of reversible smooth muscle contraction and abnormal SMC proliferation. It is yet to be understood whether this phenomenon is due to changes in the phenotype of the SMC or caused by mechanical changes in the airway wall[6], as SMC respond to their mechanical environment[3]. The increased thickness of the airway smooth muscle layer is associated with clinical severity[6], being this remodeling the cause of the airway narrowing and AHR that characterize the asthmatic condition[4].

4.2. Vascular Remodeling

The pulmonary vasculature is composed of three layers: adventitia, composed of fibroblasts; media, constituted by SMC; and intima, formed by endothelial cells[44]. During vascular remodeling all of these layers are involved.

A few hours after exposure to hypoxic conditions, the adventitial fibroblasts increase their proliferation rate, being this followed, a few days later, by hypertrophy and hyperplasia of the medial[44] and intima layers[45]. Vascular remodeling is observed not only for the large

arteries, but also arterioles, veins and microvessels, with muscle deposition around previously un-muscularized vessels. The origin of these SMC is yet to be characterized[45].

Pulmonary vascular remodeling causes an elevation of the pulmonary resistance[45] and thus pulmonary hypertension (PH), which is associated with increased morbidity and mortality in asthma patients[44].

5. Murine Models of Asthma

Animal models allow the better understanding of pathophysiological processes of human diseases in ways that would not be possible in a human being and without harming the patient. Murine models, especially those using mice, are the most commonly adopted in experimental asthma research due to the range of genetically modified strains available[24].

The induced airway abnormalities don't resemble human asthma in all aspects, since asthma does not develop spontaneously in these animals and their airways have different structural and biochemical characteristics[46]. Also, different genetic backgrounds display distinct allergic responses, as induction of airway allergy in C57BL/6 mice does not lead to the activation and accumulation of mast cells in the lung, contrary to what observed in BALB/c mice[47,48]. Nevertheless, the triggering of asthma in these mice still elicits similar effects as those observed in humans, with Th2 cytokine production, Goblet cell hyperplasia, neutrophil response followed by eosinophil response, and IgE production[49].

5.1. OVA-induced Model

The most widely used model involves systemic sensitization with intraperitoneal injection of OVA in the Th2-inducing adjuvant aluminium hydroxide (alum), followed by airway challenge with this antigen in order to develop the response[49]. These procedures can vary in the dose, frequency of sensitizations and aerosolization and duration of the latter, as well as the time point of analysis after the last challenge[46].

Sensitization with OVA can also be done via inhalation, in which an initial nasal exposure is used followed by subsequent repeated exposures to induce the allergic airway reaction. As OVA alone does not trigger the immune system, this model is dependent on the utilization of pathogen-associated patterns (PAMPs) such as bacterial LPS[46].

Although this protein induces a robust asthmatic response in mice, OVA is seldom implicated in human asthma, which led to the development of alternative models using human allergens[49].

5.2. HDM-induced Model

Contrary to the OVA, HDM is a significant source of allergens to humans, inducing atopic symptoms in susceptible individuals[50]. Airborne HDM is contaminated by LPS, an agonist of TLR4, having also other TLR agonists in its composition[50]. The interaction between HDM and these receptors in the epithelial cells is enough to initiate the immune response[46]. Therefore, HDM models involve an inhalation only procedure, where the first inhalation is succeeded by repetition of this triggering in later periods with variable dosage and duration[50].

6. Pharmacotherapy

As the fundamental role of Th2 cells in asthma is well described despite the complexity of this disease, most treatments are focused on targeting Th2 cytokines or their receptors[3]. Inhaled corticosteroids are the major drugs used in the treatment of asthma. These improve lung function and reduce the symptoms and exacerbations of the disease in patients with high Th2 cell counts[23], not being very effective in subjects belonging to the Th2-low subtype[3].

Leukotriene antagonists and inhibitors are also used in asthma therapy to block the increased vascular permeability and muscle contraction. However, these drugs show no advantages for patients with low eosinophil counts[2].

Although the aforementioned drugs are well established for the treatment of asthma, several patients don't respond to them, making their treatment a considerable challenge[3]. Continued efforts are being made to find new treatments. One example is the humanized monoclonal antibodies to IgE, currently used as a therapy, which allow the use of lower corticosteroid doses[2]. Antagonists for the major interleukins responsible for the outcomes of the asthmatic disease have also been developed, with low efficacy. Whereas anti-IL-5 antibodies have shown a contribution to the eosinophil reduction in asthmatic patients[26,40] and IL-13 antibodies seem to improve lung function in the developed clinical trials[3], IL-4 antagonists failed to show clinical efficiency[6].

Aims and Methodology

Asthma prevalence has been increasing globally, being the most common chronic lung disease in the world[2,3]. The study of the mechanisms involved in the development of this disease is therefore expanding, but still much is to be understood. Murine models of airway allergy are well established for the study of this disease, as triggering in mice elicits a similar outcome to what is observed in humans[49]. The importance of the hypoxic environment in asthma is widely accepted[7], but the cell type-specific role of the HIF pathway proteins during the asthmatic response is yet to be comprehended.

With this in mind, this project was developed with the purpose of studying to what extent modulation of the hypoxia response in T cells and myeloid cells influences the overall outcome of the disease. The studies were conducted in the PHD2 conditional-deficient mouse strain targeted in the T cell compartment (CD4:cre-PHD2$^{f/f}$ mice), as well as PHD2 and PHD2/PHD3 conditional-deficient mice in the myeloid compartment (LysM:cre-PHD2$^{f/f}$ and LysM:cre-PHD2$^{f/f}$ PHD3$^{f/f}$ mice). All mice were crossed back on a C57BL/6N background (>N9).

OVA and HDM allergy airway models were used to elicit the asthmatic response. Hallmarks of asthma were then assessed for all genotypes using several mouse, biochemical and histological methods.

The influence of the hypoxia response pathway activation in either T cells or myeloid cells on the inflammatory cell infiltration, mainly eosinophils, in the BALF and the pulmonary tissue was investigated, as eosinophilia associates with symptom scores[38].

The characterization of the asthmatic phenotype was one of the major goals of this work. As the continued stimulation of the epithelial, smooth muscle and fibroblastic cells during the development of asthma induces the remodeling of the lung tissue[3], the study of the mucus secretion by the epithelial cells, fibrosis and vascular remodeling was crucial to comprehend the severity of the disease upon deletion of hypoxia response regulators in the aforementioned immune cell populations.

Furthermore, this project aimed to illustrate the mechanism through which the hypoxia response activation in either T cells of myeloid cells contributed to the observed phenotype. As the inflammatory milieu in the lung tissue modulates the overall outcome of the disease, analysis of the pro-allergic, pro-inflammatory and anti-inflammatory cytokines in the lung was performed to further characterize the asthmatic response and therefore gain further insight in the role of this pathway in cell activity during asthma.

Materials and Methods

1. Animal Handling

1.1. Mice Strains

All mice used in this work were housed at the Medical Theoretical Centre (MTZ) at the Medical Faculty (University Hospital Carl-Gustav Carus – University of Technology Dresden, Germany), under pathogen-free conditions in individually ventilated cages (IVC) units (Techniplast) with ad libitum water and food. Experiments were performed with male and female mice between the ages of 8 to 12 weeks. All mouse lines used were born in a normal Mendelian distribution at least 9 generations backcrossed to C57BL/6N. All procedures were performed in accordance with the facility guidelines on animal welfare while approved by the Landesdirektion Dresden, Germany.

Conditional knockouts (cKO) were based on a Cre-lox system, where the Cre recombinase mediated site specific recombination between loxP sites, excising the gene region of interest (Figure 3).

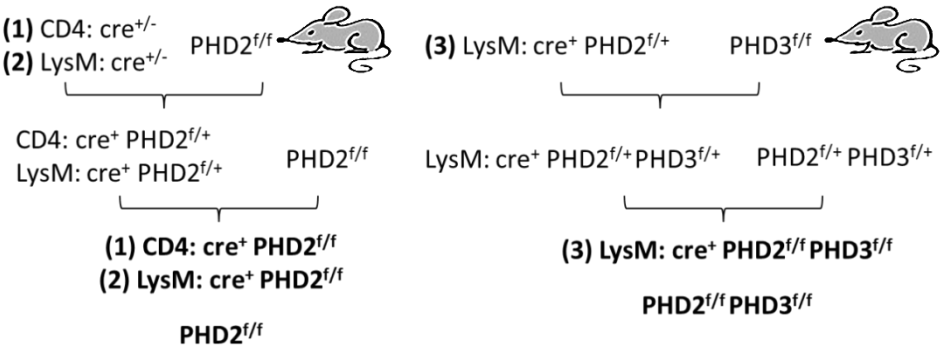

Figure 3 Breeding scheme of the mouse strains used in this work. For both the CD4:cre-PHD2$^{f/f}$ (1) and LysM:cre-PHD2$^{f/f}$ (2) strains, mice with the cre recombinase in one allele were crossed with mice expressing loxP sites encompassing the exon 2 and 3 of PHD2 in both alleles. Two crossing steps were required for the generation of these mice, as the first cross leads to, but not only, mice with excision of PHD2 in one allele. LysM:cre-PHD2$^{f/f}$ PHD3$^{f/f}$ mice (3) were obtained by the crossing of a heterozygous mouse for PHD2 in the myeloid compartment with mice expressing loxP sites flanking the exon 2 of PHD3 in both alleles. A second crossing was necessary to obtain homozygous mice lacking both PHD2 and PHD3 in the myeloid cells. The obtained cKO were analyzed versus their WT littermates; PHD2$^{f/f}$ in the case of CD4:cre-PHD2$^{f/f}$ and LysM:cre-PHD2$^{f/f}$, and PHD2$^{f/f}$ PHD3$^{f/f}$ for the LysM:cre-PHD2$^{f/f}$ PHD3$^{f/f}$. Only representative outcomes of each crossing are depicted in the figure.

CD4:cre$^{+/-}$ and LysM:cre$^{+/-}$ were crossed with mice with loxP sites upstream of exon 2 and downstream of exon 3 of PHD2 in both alleles. Two crossings allowed the generation of both CD4:cre-PHD2$^{f/f}$ (1), lacking PHD2 in the T cells, and LysM:cre-PHD2$^{f/f}$ mice (2), lacking PHD2 in the myeloid cells. To generate mice lacking both PHD2 and PHD3 in the myeloid compartment, LysM:cre-PHD2$^{f/f}$ PHD3$^{f/f}$ (3), mice obtained from the first crossing of LysM:cre$^{+/-}$ with a PHD2$^{f/f}$ mouse were used. These mice were then crossed with PHD3$^{f/f}$ mice, with loxP sites flanking the exon 2 of PHD3 in both alleles. The obtained cKO were analyzed versus their wild type (WT) littermates; PHD2$^{f/f}$ in the case of CD4:cre-PHD2$^{f/f}$ and LysM:cre-PHD2$^{f/f}$, and PHD2$^{f/f}$ PHD3$^{f/f}$ for the LysM:cre-PHD2$^{f/f}$ PHD3$^{f/f}$.

1.2. Models of Airway Allergy

5 week OVA-induced asthma model. Sensitization of the mice was performed with 3 intraperitoneal (IP) injections of 10µg OVA Grade V (Sigma-Aldrich®) and 1mg aluminum hydroxide (Sigma-Aldrich®) in 100µL phosphate buffer saline (PBS) (Gibco®) on days 0, 14 and 21. Triggering of the allergic response in the lung was done with 1% OVA in PBS inhalations on the following week (days 27 to 30). Aerosol inhalation was done inside of an IVC for 30 minutes using a JuniorBOY SX nebulizer (PARI). Mice were sacrificed on day 31 by heart extraction after washing and perfusion of the lungs (see below) (Figure 4).

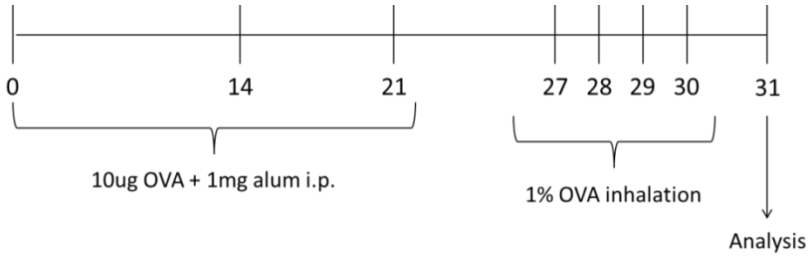

Figure 4 Time frame of the 5 week OVA-induced asthma model.

2 week OVA-induced asthma model. Mice were anesthetized with an IP injection of 100µL 0.9% NaCl (Merck) with 10mg/mL Ketamine and 1mg/mL Xylazine (Sigma-Aldrich®) and received an intranasal (IN) administration of 100µg OVA in 50µL.

12 days later an IN administration of 25µg OVA in 50uL PBS was performed, a procedure that was repeated in the following two days.

Mice were killed on day 15 as previously mentioned (Figure 5).

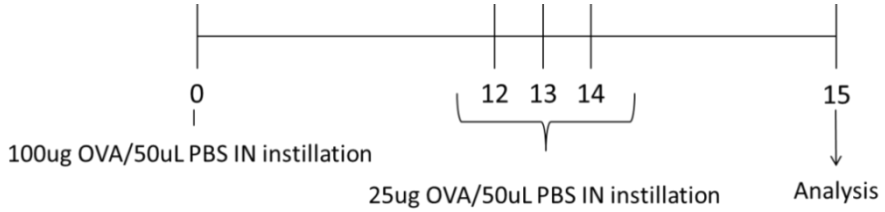

Figure 5 Time frame of the 2 week OVA-induced asthma model.

HDM-induced asthma model. Mice were anesthetized with an IP injection of 100µL Ketamine/Xylazine. 50µg of HDM extract (GREER®) dissolved in 200µL PBS was administered IN on day 0, being this procedure repeated on days 10 and 11 with a lower amount of HDM (5µg in 50µL PBS). Mice were sacrificed 3 days after the last treatment by heart removal after washing and perfusion of the lungs (Figure 6).

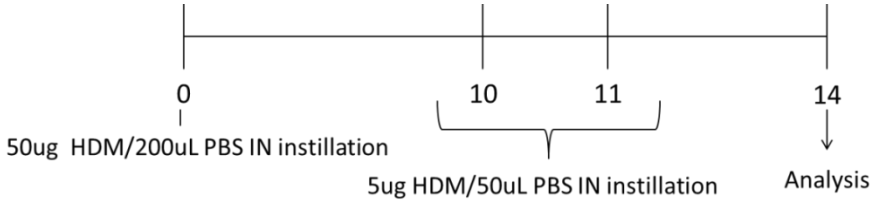

Figure 6 Time frame of the HDM-induced asthma model.

1.3. Sample Harvesting

Blood collection. Mice were anesthetized with an IP injection of 300µL Ketamine/Xylazine. Retro-orbital bleeding was performed using a capillary (BRAND®). 120µL of blood was collected into a 200µL capillary blood collection tube coated with ethylenediaminetetraacetic acid (EDTA) (KABE Labortechnik). The obtained sample was used for whole-blood analysis, and the serum utilized for the detection of IgE via an enzyme-linked immunosorbent assay (ELISA).

BALF extraction. BALF extraction is a technique commonly used to sample the epithelial lining fluid of the studied animals in order to study the influx of inflammatory cell populations after asthma induction.

After confirming the animals' lack of response to stimulation through paw pinching, the mouse was partially sterilized with 70% ethanol and a tracheostomy was performed. A small incision at the upper part of the trachea was used to expose the sternohyoid muscle, which was then cut longitudinally to reveal the trachea. This structure was punctured with a Vasofix® cannula (Braun Medical) and 200µL of ice-cold PBS was injected into the lungs using a

1mL syringe (BD™). This volume was aspirated and collected in a 2mL Eppendorf tube (Sarstedt) placed on ice. The lavage was repeated for a total volume of 2mL. This procedure yielded approximately 1.8mL of BALF.

Lung digestion. Digestion of the lung was performed in order to study the inflammatory cell populations as well as the $CD4^{+}$T cell subsets present in the tissue.

To obtain single-lung-cell suspensions, lungs were first perfused with 20mL PBS through the right ventricle using a 22G needle (BD™). In the 5 week model, perfusion was firstly done with 20mL sodium nitroprusside dehydrate (Sigma-Aldrich®), a vasodilator used in order to better remove the blood from the tissue. 150mg of lung tissue was then cut into small pieces and digested for 30 minutes in 6-well plates (Corning® Costar®) at 6 g at 37ºC in PBS 20% Collagenase A (10mg/mL, Roche) and 0.5% DNAse (Roche). Digestion was stopped with 400µL of PBS/5% fetal bovine serum (FCS) (Biochrome)/4mM EDTA (Carl Roth)/0.5% DNAse. The supernatant was then filtered and the resulting suspension was used for flow cytometry.

Lymph node extraction. The lymphatic system is actively involved in immune responses to foreign antigens. Therefore, the study of the characteristics of the lymphocytes residing in the lymph nodes provides information regarding the activation status of the T cells triggered by the lung DCs that migrate into these organs.

The mouse skin was peeled from the forepaws and the brachial lymph nodes were collected using a tweezer. These organs were manually disrupted using frosted slide ends (Engelbrecht) into 2mL PBS/5%FCS and the ensuing cell suspension was then filtered into a 2mL Eppendorf tube and used for flow cytometry.

2. Inflammatory Cell Analysis

2.1. Cytospin

Cytospin is a method commonly used to concentrate the cells present in the sample on a restricted area of a slide, so that these can be stained and morphologically examined. It requires the use of a cytocentrifuge, that provides the centrifugal force required to gently fix the cells on the glass.

150µL of BALF was inserted into reusable cytofunnels (Thermo Scientific) which were assembled over pre-labelled slides covered by a filter paper. These chambers were inserted

into a cytospin 3 cytocentrifuge (Shandon) and spun at 150 g for 8 minutes, with the acceleration of the rotor put to minimum. Slides were then carefully removed from the cytofunnels and allowed to dry.

May-Grünwald-Giemsa Staining. May-Grünwald-Giemsa staining was performed on cytospins to allow identification of the various hematopoietic cells present in the BALF. Slides were placed in May-Grünwald Stain (Merck) for 3 minutes. This stain consists of a mixture of eosin, which is acidic, and methylene blue, which stains the acidic components of the cell. After this period, the samples were immersed in buffer solution pH 6.8 (Merck) for 5 minutes and then placed in diluted Giemsa solution (Sigma-Aldrich®) diluted 20 times in buffer solution for 20 minutes. Giemsa has specificity for the phosphate groups of DNA, staining the nucleus of cells in a purple color. The slides were then rinsed in buffer solution, allowed to dry and covered with a coverslip (Engelbrecht) using M Glass (Merck).

2.2. Flow Cytometry

2.2.1. Surface Staining

Lung and BALF. All single-cell suspensions obtained from either BALF or digested lung tissue were stained for myeloid and lymphoid populations. Centrifugation of the samples was done at 145g for 7 minutes. The obtained pellet was re-suspended in 500µL PBS/5% FCS/4mM EDTA/0.5% DNAse. From this volume, 100µL of sample was loaded into a 96-well, V-bottom plate (Corning® Costar®). Samples were spun down at 402g for 2 minutes and incubated in 50µL of antibody mix for 30 minutes on ice under dark.

The myeloid staining mix included antibodies against CD45 (30-F11, eBioscience®), used to identify leukocytes while excluding erythrocytes and platelets; CD11b (M1/70, BD™), the C3 complement receptor, expressed highly in monocytes and macrophages, but also to a lower extent in granulocytes and some subsets of DCs; CD11c (HL3, BD™), primarily expressed in DCs, but also in AMs; sialic acid-binding immunoglobulin-like lectin F (Siglec-F) (E50-2440, BD™), an inhibitory receptor on the surface of eosinophils, also expressed on the surface of AMs; Ly6G (1A8, eBioscience®), expressed at the surface of peripheral neutrophils; F4/80 (BM8, eBioscience®), a macrophage surface marker; and MHC Class II (AF6-120.1, BioLegend®), present on the surface of antigen-presenting cells (APCs), such as macrophages and specially DCs, and whose expression is increased after antigen processing by these cells. 4',6'diamidino-2-phenyldole (DAPI) (Life Technologies™) was used in order to assess the cell

viability, as this fluorescent binds to DNA and fluoresces as the membrane integrity of dead cells is compromised.

The lymphoid staining mix was composed of antibodies against CD45; CD45R (B220) (RA-6B2, eBioscience®), an epitope mainly expressed by the B cell lineage; CD3 (145-2C11, eBioscience®), a complex that is required for assembly, trafficking and expression of the T-cell receptor (TCR), being expressed at the surface of T cells; CD4 (GK1.5, eBioscience®), a co-receptor of the TCR expressed by Th cells; and CD8 (H35-17.2, eBioscience®), a co-receptor of the TCR found at the surface of T cytotoxic cells. DAPI was used as an indicator of cell viability.

After staining, samples were spun at 402g for 2 min and re-suspended with 300µL PBS/5%FCS/4mM EDTA/0.5% DNAse.

Lymph nodes. Lymph node single-cell suspensions were stained for lymphocytic populations. Briefly, samples were spun for 7 minutes at 402g and the obtained pellet was re-suspended in 1mL PBS/5% FCS/4mM EDTA/0.5% DNAse. From this volume, 150µL of sample was loaded into a 96-well plate, V-bottom and a surface staining procedure already described was performed.

The antibody mix consisted of antibodies against CD3 (eBio500A2, eBioscience®), CD4 (GK1.5, eBioscience®), and CD8 (53-6.7, eBioscience®) in order to identify the T cell populations. Anti-CD19 antibody (MB19-1, eBioscience®) was used to identify B cells, as this molecule associates with their B cell receptor. Anti-CD69 antibody (H1.2F3, eBioscience®) was used in order to identify recently activated cells; CD62L (L-selectin) (MEL-14, BioLegend®) was used as a marker for naïve lymphocytes. DAPI was used as an indicator of cell viability.

2.2.2. Intracellular staining

T cell subsets. Th cells can differentiate into several subtypes, which have distinct transcription factors regulating their activity. The study of the Th cell subpopulations in asthma allows the analysis of the PHD2-mediated T helper cell polarization.

100µL of lung cell suspension was used for this staining in a 96-well plate, V-bottom. After centrifugation at 402g for 2 minutes, samples were stained with antibodies against the surface markers CD45 (30-F11, eBioscience®), CD3 (145-2C11, eBioscience®) and CD4 (GK1.5, eBioscience®). Staining lasted 30 minutes and was done at 4ºC in the dark.

After the surface staining, cells were washed with PBS. The intracellular staining was done using the Foxp3 / Transcription Factor Staining Buffer Set (eBioscience®). 200µL of FoxP3 Fixation/Permeabilization solution diluted with diluent (1:4 vol/vol) was added to each well and samples were left incubating in the dark overnight.

200µL of permeabilization buffer diluted with distilled water (1:10) was added to each well after centrifugation at 226g for 2 minutes. 3µL of each intracellular antibody was added to each well in 100µL permeabilization buffer. FoxP3 (FJK-16s, eBioscience®) was used as a marker for Treg cells, whereas GATA3 (TWAJ, eBioscience®) was used in order to identify the Th2 subset. The staining was done for 30 minutes under dark conditions at 4ºC. Samples were washed twice and then re-suspended in 300µL of PBS for flow cytometric analysis.

2.2.3. Compensation controls

Compensation controls for every staining were done using OneComp eBeads (eBioscience®) or fixed single-bone marrow cell suspensions in case of the intracellular staining. For the latter, a femur was removed from one mouse and flushed with 2mL of PBS/5%FCS using a 23G needle (BD™). The obtained suspension was then filtered and centrifuged for 2 min at 402g. Cells were fixed using the same protocol as mentioned for the intracellular staining.

Flow cytometric analysis was performed on LSR II Flow Cytometer (BD™) and data was analyzed using FlowJo Version 10 software (TreeStar). All used antibodies and respective target cells are summarized in Table 1. Gating strategies of the myeloid, lymphoid and lymph node staining are depicted in Figures 38, 39 and 40 of the Appendix, respectively.

Table 1 Antibodies used in this work and their respective target population.

Antibody	Target population
CD45 – FITC (clone 30-F11)	Leukocytes
CD11b – AmCyan (clone M1/70)	Monocytes and Macrophages
CD11c - APC-cy7 (clone HL3)	DCs and AMs
Siglec-F – PE (clone E50-2440)	Eosinophils and AMs
Ly6G- APC (clone 1A8)	Neutrophils
F4/80 - PE-cy5 (clone BM8)	Macrophages
MHC II – PE-cy7 (clone AF6-120.1)	APCs
B220 – PE-cy7 (clone RA-6B2)	B cells
CD3-APC (clone 145-2C11) CD3 – Alexa Fluor 700 (eBio500A2)	T cells
CD4 – PE (clone GK1.5)	Th cells
CD8 – PE-cy5 (clone H35-17.2) CD8 – PE-cy7 (53-6.7)	Cytotoxic T cells

CD19 – FITC (clone MB19-1)	B cells
CD69 – APC (clone H1.2F3)	Activated lymphocytes
CD62L – PerCP (clone MEL-14)	Naïve lymphocytes
FoxP3 - Alexa Fluor® 488 (clone FJK-16s)	Treg cells
GATA3 - eFluor® 660 (clone TWAJ)	Th2 cells
DAPI	Dead cells

2.2.4. Cell Quantification

Absolute cell numbers in BALF, lung and lymph nodes. Total cell counts were obtained through MACS Quant (Myltenyi) measuring. 10µL of sample was loaded into a 96-well plate, flat bottom (Corning® Costar®) in 90µL of PBS/5%FCS/0.1% DAPI. 1µL of anti-CD45 was added to each well. The samples were incubated for 30 minutes under dark conditions at 4ºC. This method allows the enumeration of the absolute number of live cells that express the CD45 surface marker, providing for total numbers of each cell population analyzed in flow cytometry. The acquired results were examined using FlowJo Version 10 software (TreeStar).

Whole blood analysis. Blood parameters were determined using an automated blood cell counter XT-4000 (Sysmex). Platelet counts, hemoglobin and hematocrit concentration and white and red blood cell numbers in circulation were measured, as well as lymphocyte, monocyte, eosinophil and neutrophil numbers. 40µL of blood was diluted 1:5 in 0.9% saline solution for measurement. The remaining blood was centrifuged at 502g for 2 min and the plasma was collected and stored at -80ºC until an IgE ELISA was performed.

3. Biochemical Analysis

3.1. Lung Tissue Analysis

Lung tissue was obtained for cytokine analysis by ELISA and electrochemiluminescence (ECL). The tissue was homogenated in 500µL of cOmplete Protease Inhibitor (Roche) in PBS/0.05% Tween-20 (VWR®), centrifuged at full speed for 10 minutes and the supernatant was collected.

Bradford assay. A Bradford assay was performed for total protein concentration measurement. This colorimetric protein assay relies on the absorbance shift of the Coomassie Blue dye when bound to proteins in the sample.

25uL of each sample was used to prepare successive dilutions (1:5) of the sample in PBS/0.05% Tween-20/% cOmplete. A bovine serum albumin (BSA) standard (2mg/mL) (Thermo Scientific) was diluted in the same diluent, with successive two-time dilutions to a final concentration of 125mg/mL. 250µL of Bradford Reagent (Bio-Rad) was loaded into a 96-well plate, flat bottom. From either sample, standard or diluent, 5µL was loaded to each well. Absorbance was measured at 595nm using a Synergy™HT Reader (BioTek). After analysis of total protein content, 30 to 50µg of protein was used for cytokine measurement.

IL-5 and IL-13 ELISA. An ELISA is an analytic biochemical assay that involves the detection of an antigen of interest through binding with a set of specific antibodies followed by the enzymatic cleavage of a substrate. Sandwich ELISAs ensure specificity of the obtained signal by the use of an antibody against the antigen that binds it to the surface of the polystyrene plate (capture antibody) and a second antibody against this substance that is biotinilated (detection antibody), assuring binding with the enzyme used for the color reaction which in turn is bound to Avidin, a tetrameric biotin-binding protein.

Mini ELISA Development Kits (Peprotech®) were used for the IL-5 and IL-13 ELISAs. High-affinity binding 96-well flat bottomed plates (Greiner Bio-One) were coated overnight at room temperature with 100µL capture antibody in PBS. After washing of the plate 4 times with 0.05% Tween-20 in PBS, blocking of the plate was done for one hour with 300µL PBS/1%BSA (Sigma-Aldrich®). After washing, the respective volume of each sample and standard was added to the plate and successive dilutions (1:3) were performed for every sample. Dilutions were made in PBS/0.05% Tween-20/0.1%BSA. Incubation with the samples lasted 2 hours, followed by 4 washing steps. 100µL of detection antibody was added and the plate was left incubating for another 2 hours. 100µL of Avidin-horseradish peroxidase (HRP) conjugate (1:2000) was used and 2,2'-azino-bis(3-ethylbenzothiazoline-6-sulfonic acid) (ABTS) Liquid Substrate Solution (Sigma-Aldrich®) was then added after washing for color development. Optical density (O.D.) was measured after 30 minutes at 405nm with a wavelength correction at 650nm with a Synergy™HT Reader (BioTek).

ECL assay. An ECL assay is a highly sensitive sandwich immunoassay used to measure the levels of particular protein targets in a single sample. This technique is based on the principle that under an appropriate chemical environment, the application of a voltage to the

solution leads to the excitation of the electrochemiluminescent labels used, which emit light upon relaxation. Multiple labels can be coupled to the proteins in the sample, from which the instrument measures the intensity of emitted light in order to quantify the particular proteins of interest in the sample.

A Proinflammatory Panel 1 (mouse) Kit (MSD®) was used to measure the concentration of IL-10, an anti-inflammatory cytokine mainly produced by monocytes and Treg cells; IL-1β, a pro-inflammatory cytokine produced by activated macrophages; IL-4, mainly produced by Th2 cells; IL-6, a pro-inflammatory cytokine mainly produced by Th1 cells and macrophages; and TNF-α, also pro-inflammatory and produced mainly by macrophages.

Lung tissue homogenate was diluted in Diluent 41, provided in the kit, to a final concentration of 0.6mg/mL. The standard was successively diluted (1:2) in Diluent 41, according to the manufacturer's instructions. From either sample or standard solutions, 50µL was added to the plate, which was left incubating at room temperature with shaking for 2 hours. The plate was washed 3 times with 200µL PBS/0.05% Tween-20 and 25µL of antibody solution including antibodies for all of the above mentioned cytokines was added to each well. Incubation with the antibody mix lasted 2 hours under the same conditions as for the samples, the wells were washed and 150µL of Read Buffer T in deionized water (1:2) were added to each well just prior to measuring. Measurement of the plate was done on a QuickPlex SQ 120 (MSD®) and analysis of the results was carried out using the MSD Discoveery Workbench® analysis software (MSD®).

3.2. Plasma Analysis

IgE ELISA. A Mouse IgE Ready-SET-Go!® (eBioscience®) kit was used in order to measure IgE levels in the plasma obtained from the retro-orbital bleeding. The high-affinity 96-well plate was coated with capture antibody overnight at 4ºC. Washing was done twice with 0.05% Tween-20/PBS and the plate was blocked with 250µL of blocking buffer prepared according to the manufacturer's instructions for 2 hours. Next, the plate was washed as described previously and samples/ standards were diluted in the Assay Buffer A provided by the kit and added to the wells. Incubation lasted 2 hours, after which the plate was washed and incubated with 100µL of detection antibody for another hour at room temperature on a microplate shaker PMR-30 (Grant) at 30 oscillations per minute. 100µL of streptavidin-HRP were used as the reporter and incubation with this complex was done for 30 minutes. The plate was washed another 4 times and 100µL of Substrate Solution provided in the kit was added to each well, and incubated for 15 minutes. The reaction was stopped by adding 100µL

2M sulfuric acid (H_2SO_4). The plate was read at 450nm with a wavelength correction at 570nm using a Synergy™HT Reader (BioTek).

4. Histological Analysis

4.1. Tissue Preparation

Histological analysis of the lung tissue allows for a quantification of the degree of disease in each individual animal. This technique is used to measure tissue alterations and remodeling that are the result of the asthmatic triggering.

Lung tissue was collected from each mouse and fixed overnight in 4% Paraformaldehyde (PFA) (Carl Roth) at 4ºC. Samples were then processed in order to remove the water from the tissue and replace it with paraffin. Briefly, samples were transferred through baths of progressively higher ethanol concentrations, being then immersed in xylene and, subsequently, paraffin wax. Embedding was done using a TES Valida (MEDITE), where samples were placed into molds and covered with paraffin externally. 2µm cross sections of the blocks were cut using a RM 2235 microtome (Leica) and mounted on glass microscope slides.

As the staining solutions used are aqueous, sections were rehydrated prior to staining. Samples were passed through Roticlear (Carl Roth), a xylene alternative used as a clearing agent, for 15 minutes, followed by 5 minute incubation in decreasing strengths of ethanol (100/90/80/70%). Finally sections were incubated in distilled water.

Upon completion of all performed stainings (see below), all slides were washed, dehydrated and incubated in Roticlear for 15 minutes. Mounting was done with VectaMount (Vector Laboratories) and a coverslip was placed on top to protect the samples.

4.2. Histological Staining

Haemotoxylin and Eosin (H&E) Staining. H&E is one of the most commonly used histological staining, involving the use of an acidic (Eosin) and a basic dye (Haematoxylin). Eosin stains basic structures, such as the cytoplasm of cells and protein structures, in pink; whereas the latter stains acidic structures, such as the nucleus of cells, in a purplish blue. This staining was used in order to assess cell infiltration in the lung tissue.

After rehydration, the slides were immersed in Mayers Haematoxylin (SAV Liquid Production) for 5 minutes. Warm water was used to rinse the samples, which were then submerged in Eosin (Klinik Apotheke) for 3 minutes.

Periodic Acid Schiff (PAS) staining. PAS staining is a method used to detect polysaccharides, glycoproteins and mucins in tissues. Periodic acid oxidizes these sugars, forming aldehydes that react with the Schiff reagent, giving a dark pink color. Haematoxylin is then used as a counterstain and the final outcome is used to assess mucus production by the Goblet cells in the bronchi of the tissue.

Slides were incubated in 2% Periodic Acid (VWR) for 15 minutes. After a short immersion in distilled water, all slides were transferred to a Schiff Reagent (SAV Liquid Production) container, where they were left submerged for 20 minutes. Washing was done with water and samples were counterstained for 5 minutes in Mayers Haematoxylin.

Masson Trichrome (MT) staining. This particular staining was performed in the Institute of Pathology of the University Hospital Carl Gustav Carus. This staining allows the distinction between cells and the surrounding connective tissue, involving the usage of three solutions that stain the nuclei and the cytoplasm of the cells and the collagen fibers. The final result leads to the cell staining in red, while the collagen fibers are stained in blue, allowing the quantification of the fibrous area of the tissue.

4.3. Microscopy

Light microscopy was done with an Axioplan-2 imaging microscope (Carl Zeiss). The cameras and acquisition software were Axiocam MRc5 and Axiovision. Image processing and analysis was done using ImageJ version 1.47V.

5. Statistical Analysis

Data and graphs represent mean ± SEM of representative experiments. Statistical significance was calculated as two-tailed by Students t-test (GraphPad Prism v6®), with $p<0.05$ considered statistically significant.

Results and Discussion

1. Induction of the Asthmatic Response

1.1. Inflammatory cell Infiltration Analysis

In order to induce an asthmatic phenotype in the studied mice, a 5 week model of OVA-induced pulmonary inflammation was first applied. Morphological examination of the infiltrating inflammatory cells in the BALF was performed using cytospin and May-Grünwald-Giemsa staining (Figure 7). Nuclei are stained with a dark purple color due to the staining with the basic dye, while the cytoplasm stains light blue or pink due to the low concentration of nucleic acids.

Untreated WT mice showed little cell amounts in the BALF, being the major population in this sample cells with a small nucleus to cytoplasm ratio, which correspond to the AM population, present in the airway under steady state conditions. AMs represent the majority of cells in the airway in healthy mice[35] and these macrophages have extensive cytoplasmic areas (Figure 7A). As the junctions between epithelial cells in the bronchi of asthmatic mice are loosened, washing of the airway in triggered mice allows the extraction of inflammatory cells that migrate through these structures into the alveolar space to defend the organism against the inhaled antigen. Therefore, in asthmatic mice a high cell infiltration was observed in the BALF, composed mainly of various inflammatory cell types with very distinct morphologies (Figure 7B).

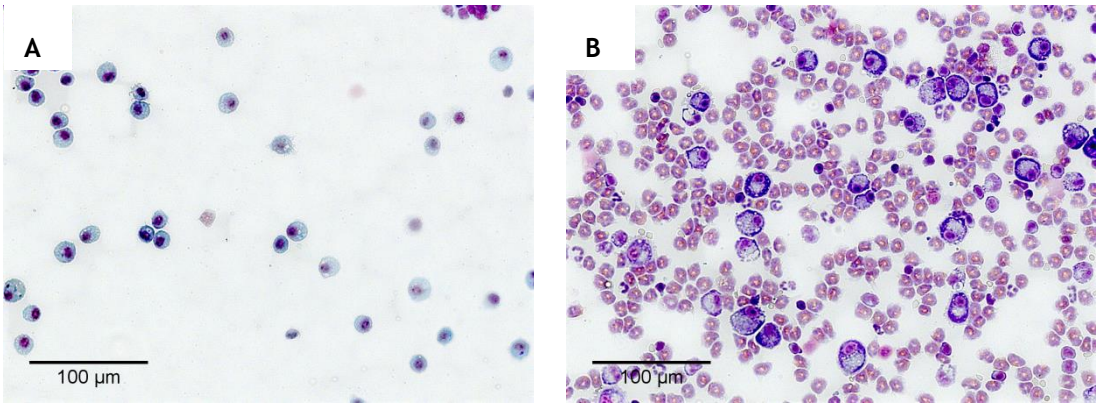

Figure 7 May-Grünwald-Giemsa staining of the cytospin obtained from inflammatory cells in the BALF of untreated (A) or OVA-treated mice (B). Cells nuclei are stained with a dark purple color, being the cytoplasm light blue or pink due to the low concentration of nucleic acids.

Several inflammatory cells are involved in the pathology of asthma. Activation of the T cells in the lymph nodes by the DCs leads to their migration into the lung tissue and consequent recruitment and activation of downstream inflammatory cells such as eosinophils and neutrophils[6].

Analyzing samples from asthmatic mice under higher magnification, gave the possibility to characterize the aforementioned populations and therefore identify the infiltrating cells in the BALF under allergic airway conditions (Figure 8).

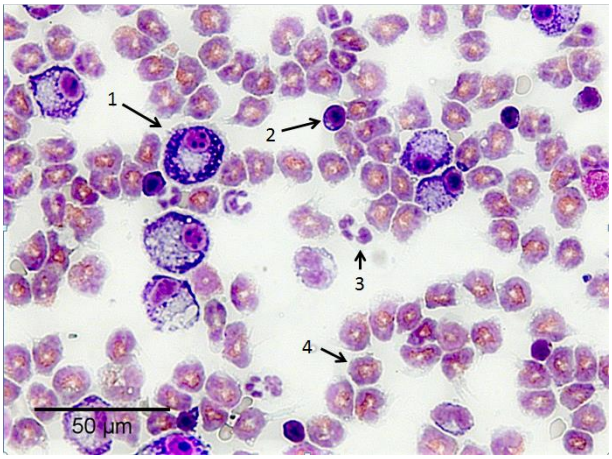

Figure 8 May-Grünwald-Giemsa staining of the cytospin obtained from inflammatory cells in the BALF of OVA-treated mice. Infiltration of several distinct cell populations was observed, mainly AMs (1), lymphocytes (2), neutrophils (3) and eosinophils (4).

AMs and lymphocytes both display a single one-lobed nucleus, but the first possess big cytoplasmic area comparing to their nuclear space (1), while the second show a large nucleus to plasma ratio (2). Eosinophils and neutrophils, however, are polymorphonuclear cells, showing lobed nucleus, which makes them easily distinguishable from the other cell types. While the neutrophil cytoplasm is stained in pale blue (3), eosinophil granules, which are alkaline, are stained in orange (4) due to the binding of eosin to these structures (Figure 8). Analyzing the cell populations in the BALF from triggered mice, the eosinophil population arose as the major cell type in the samples. This cell population produces cytokines and other mediators that contribute to the pathology of asthma[25], being the migration of these cells into the lung during asthma correlated with symptom scores[38]

1.2. Mucus Production in the Lung

During asthma, there is an induction of the remodeling of the lung tissue. As a response to the damage of the epithelium, epithelial cells proliferate and differentiate into Goblet cells, which are mucus-producing cells[6]. In healthy epithelium (Figure 9A), mucus production is negligible. However, after asthma induction, it is possible to observe the presence of Goblet cells in the epithelium that stain for PAS, turning dark pink (Figure 9B). Mucus production by Goblet cells has a protective purpose, as this substance traps antigens in the airway space, not allowing their invasion onto the tissue. However, the production of mucus by the epithelial cells in the lung during asthma is excessive and can contribute to the airway obstruction observed in asthmatic patients[4].

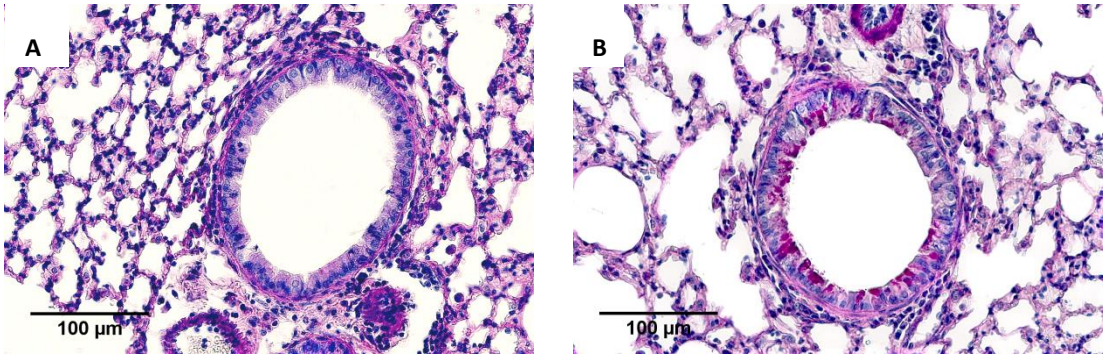

Figure 9 PAS staining of sections from either untreated WT (A) or WT-triggered (B) lung. Mucins are stained in dark pink and associate with the presence of Goblet cells in the bronchus.

The asthmatic triggering was performed on WT mice, as well as on cKO mice for PHD2 in either the T cells, CD4:cre-PHD2$^{f/f}$, or the myeloid cells, LysM:cre-PHD2$^{f/f}$. To assess if the responsiveness to the OVA-treatment was affected by the deletion of PHD2 in either the T cell or myeloid cell compartment, the mucus production in the bronchi of asthmatic mice was analyzed. As histology gives a clear indication of the severity of the phenotype, quantification of the Goblet cell coverage in bronchi of lungs from each genotype was performed (Figure 10).

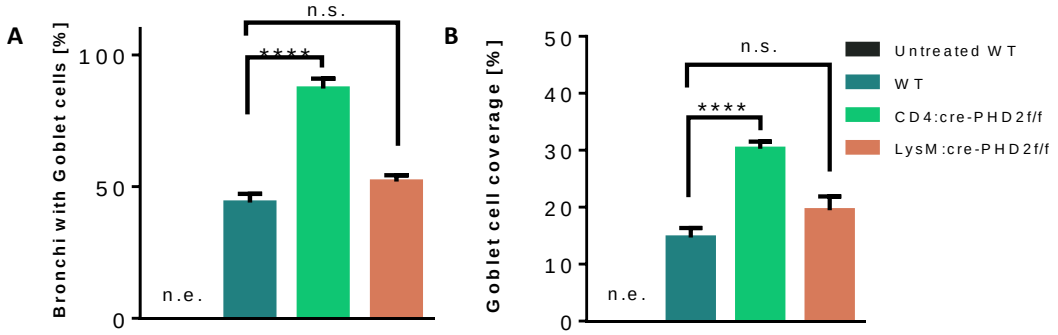

Figure 10 Goblet cell quantification in lung sections from untreated WT (n=8), WT-triggered (n=18), CD4:cre-PHD2$^{f/f}$-triggered (n=15) and LysM:cre-PHD2$^{f/f}$-triggered mice (n=6). The percentage of bronchi expressing Goblet cells (A) and the overall Goblet cell coverage in the lung (B) were measured. Data are presented as mean ± SEM. n.e. – not expressed; n.s. – not significant; ****p<0.0001.

The epithelial remodeling was observed for all genotypes, with approximately 44% (±14%) of the bronchi in the tissue expressing Goblet cells (Figure 10A) and with an increase of Goblet cell coverage from zero up until approximately 15% (±7%) in asthmatic WT mice (Figure 10B). A significant increase in the percentage of bronchi expressing the Goblet cells and total Goblet cell coverage in the lung tissue was observed for the CD4:cre-PHD2$^{f/f}$ mice in comparison with the WT-triggered mice. This indicates a more severe asthma phenotype. No significant differences were observed between the WT-treated and the LysM:cre-PHD2$^{f/f}$-treated mice.

Given the higher susceptibility of the CD4:cre-PHD2$^{f/f}$ to asthma, this genotype was further analyzed for other tissue remodeling parameters, as well as inflammatory cell numbers in BALF and lung tissue and cytokine concentration.

2. The Role of PHD2 in T cells during Asthma

2.1. 5 week OVA-induced Asthma Model

2.1.1. Tissue remodeling evaluation

Epithelial cell proliferation subsequent to cytokine stimulation upon asthma is one of the major causes for the bronchoconstriction observed in asthmatic patients. The proliferating cells can give rise to Goblet cells, increasing the mucus production in the bronchi and aggravating the disease outcome[3,6]. To analyze the proliferation of epithelial cells in both OVA-treated groups, the ratio between the luminal area and the total bronchi area was quantified (Figure 11).

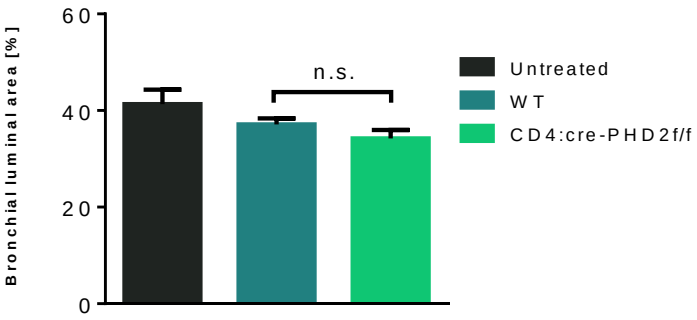

Figure 11 Bronchial luminal area quantification of CD4:cre-PHD2$^{f/f}$ mice in the 5 week OVA-induced asthma model. Lung sections from untreated WT (n=5), WT-triggered (n=16) and CD4:cre-PHD2$^{f/f}$-triggered (n=13) were analyzed using ImageJ. Bronchial luminal area is expressed as the ratio between the lumen area and the total area of the bronchus. Data are presented as mean ± SEM. n.s. – not significant.

No differences in bronchial thickness were observed between triggered and untreated mice. As Goblet cell coverage was observed for all OVA-treated mice, with a significant increase in the CD4:cre-PHD2$^{f/f}$ mice comparing to the WT, this could indicate that these cells are being originated from metaplasia and not hyperplasia of the cells of the epithelium.

During asthma, there is an increase in collagen deposition surrounding the bronchi, as the result of the continued stimulation of fibroblasts by the pro-fibrotic mediators produced by the damaged epithelium[6]. Therefore, this parameter was investigated in the asthmatic WT and CD4:cre-PHD2$^{f/f}$ mice, as the latter showed a stronger phenotype in the Goblet cell presence in the bronchi (Figure 12).

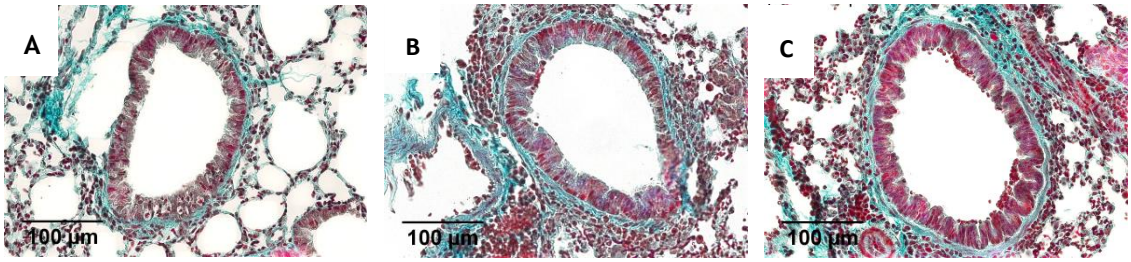

Figure 12 Masson Trichrome (MT) staining of sections from either untreated WT (A), WT-triggered (B) or CD4:cre-PHD2$^{f/f}$ lung (C). Collagen fibers are stained in a blue color, allowing the quantification of the fibrous area of the tissue.

Comparing the bronchi from untreated (Figure 12A) with OVA-treated mice (Figure 12B), it is possible to observe a higher collagen deposition surrounding this structure upon asthmatic triggering. This feature is maintained for the CD4:cre-PHD2$^{f/f}$ mice triggered with OVA (Figure 12C) and represents one of the major hallmarks of the disease. Collagen fibers are stained in blue, being easily distinguishable from the cells, stained in red. The proportion of the collagen area in proportion to the bronchial area was quantified for each sample using ImageJ (Figure 13).

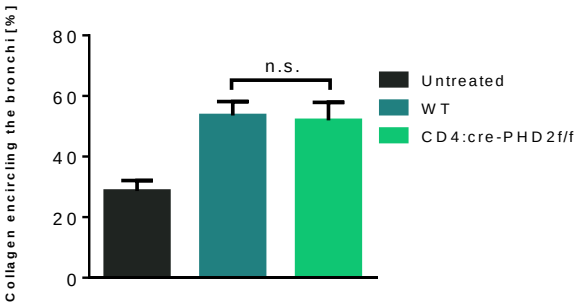

Figure 13 Quantification of the collagen deposition surrounding the bronchi in CD4:cre-PHD2$^{f/f}$ mice in the 5 week OVA-induced asthma model. Lung sections from untreated WT (n=5), WT-triggered (n=16) and CD4:cre-PHD2$^{f/f}$-triggered (n=13) were analyzed using ImageJ. Collagen encircling the bronchi is expressed as the ratio between the collagen-covered area and the area of the bronchial wall. Data are presented as mean ± SEM. n.s. – not significant.

An increase in collagen deposition surrounding the bronchi occurs after treatment with OVA, confirming the asthmatic phenotype; however, no differences were observed between genotypes.

The fibrotic changes in the lung tissue are a downstream effect of the alterations observed in the lung epithelium, as well as TGF-β production by the inflammatory cells[6]. Thus, the comparable deposition of collagen between genotypes can be the result of an equal pro-fibrotic mediator production by the epithelial cells as well as a plateaued production of TGF-β by the immune cells invading the lung, which should be confirmed via ELISA.

Vascular remodeling in the lung occurs under hypoxic conditions and leads to a heightening in pulmonary resistance. All cell layers of the vessels increase their proliferation rates, resulting in a reduction in the luminal area of the vessel[44] (Figure 14).

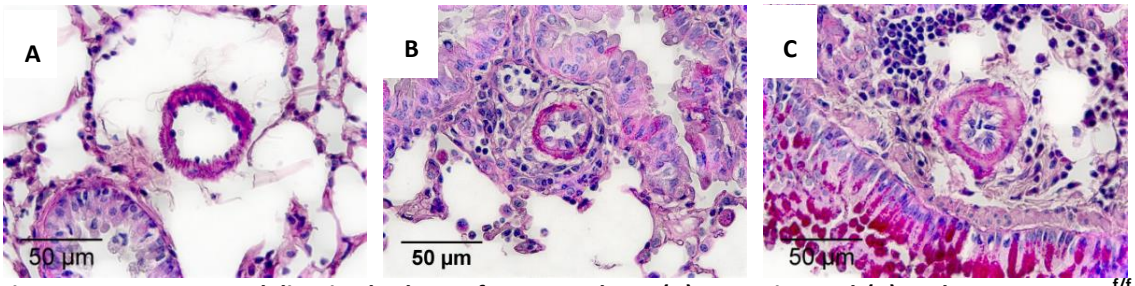

Figure 14 Artery remodeling in the lung of untreated WT (A), WT-triggered (B) and CD4:cre-PHD2$^{f/f}$ mice (C). The SMC in the media layer are stained in pink, being the endothelial cells in the intima marked in purple.

Under steady state conditions (Figure 14A) arteries present a high lumen/vessel ratio, being the arterial wall thin and very well delimited. However, in both WT (Figure 14B) and CD4:cre-PHD2$^{f/f}$ (Figure 14C) mice it is possible to observe a thickening of the SMC layer, as well as proliferation of the endothelial cells to the interior of the arterial lumen, consistent with vascular remodeling. The ratio between luminal area and vascular area was quantified for both asthmatic groups using ImageJ (Figure 15).

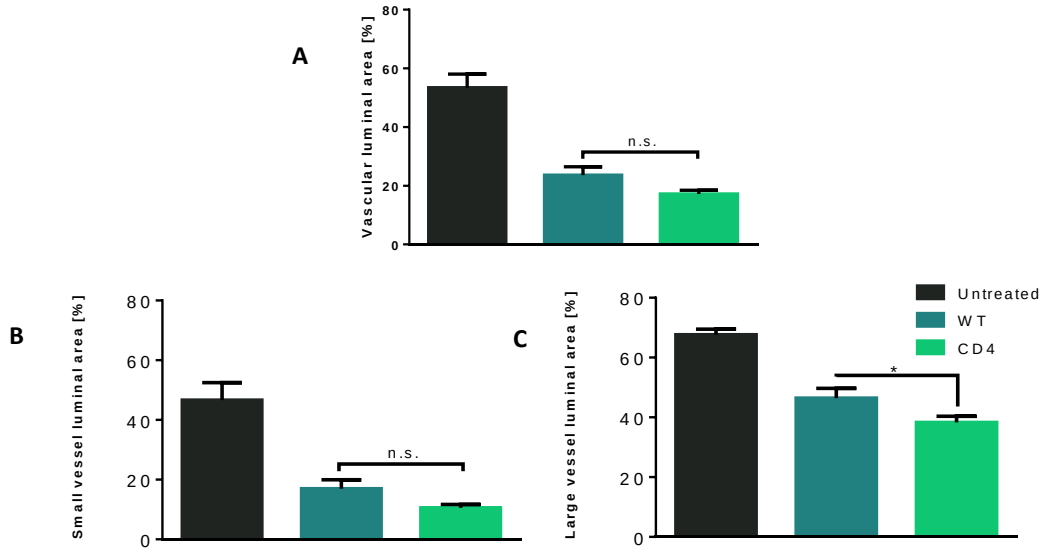

Figure 15 Quantification of the vascular remodeling in the lung in CD4:cre-PHD2$^{f/f}$ in the 5 week OVA-induced asthma model. Lung sections from untreated WT (n=5), WT-triggered (n=18) and CD4:cre-PHD2$^{f/f}$-triggered (n=16) were analyzed using ImageJ. Vascular luminal area is expressed as the ratio between the lumen area of the vessel and the total area of the vessel. Small vessels depict vessels with a total area smaller than 10mm^2, being the large vessels of sizes above the aforementioned. Data are presented as mean ± SEM. n.s. – not significant; *p<0.05.

In both WT and CD4:cre-PHD2$^{f/f}$ mice, there was a significant reduction in vascular lumen (Figure 15A), for both vessels with an area smaller than 10mm^2 (Figure 15B) and large vessels (with an area higher than 10mm^2) (Figure 15C). There is a trend for a lower luminal fraction in the vessels of the CD4:cre-PHD2$^{f/f}$ mice comparing with the WT, which is only significant for larger structures (Figure 15C). The vascular remodeling in the asthmatic mice from both groups causes an increase in pulmonary resistance and represents a hindrance in lung perfusion, leading to the need of a vasodilator and limiting the inflammatory cell quantification in the tissue due to possible contamination with blood.

2.1.2. Inflammatory cell infiltration analysis

As the asthmatic phenotype seemed to be more aggravated in the CD4:cre-PHD2$^{f/f}$ mice, inflammatory cell infiltration was assessed for both BALF and lung tissue using flow cytometry (Figure 16). This technique allowed obtaining relative as well as absolute cell numbers of each leukocyte population.

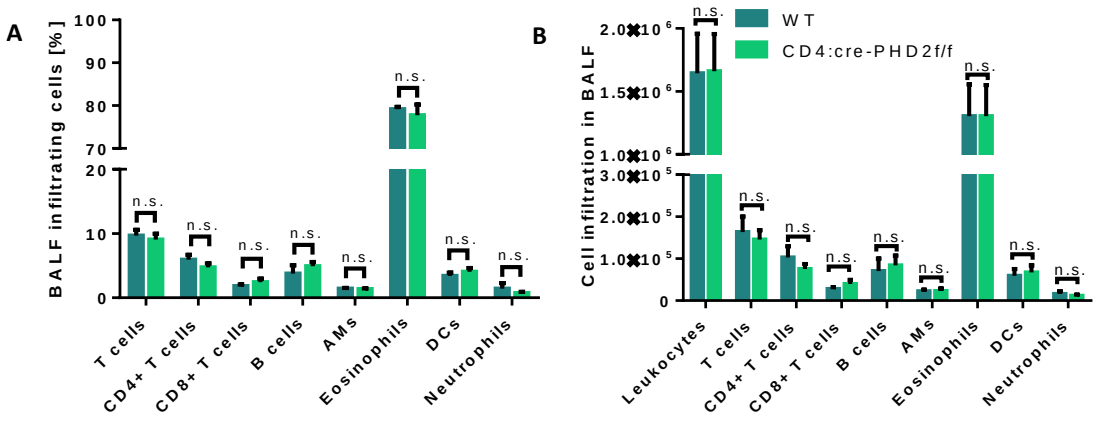

Figure 16 Inflammatory cell infiltration in the BALF of CD4: cre PHD2$^{f/f}$ mice in the 5 week OVA-induced asthma model. The percentage (A) or total counts (B) of each leukocyte cell population were assessed by flow cytometry in the BALF of WT-triggered (n=4) and CD4:cre-PHD2$^{f/f}$-triggered mice (n=4). Data are presented as mean ± SEM. n.s. – not significant.

Although the mucus production is more exacerbated in the CD4:cre-PHD2$^{f/f}$ mice, with a tendency for higher vascular remodeling when comparing with WT littermates, no differences in inflammatory cell infiltration exist between these groups in either percentage (Figure 16A) or absolute number of cells (Figure 16B). The lack of differences between genotypes might indicate that at the analyzed time point the infiltration of cells into the BALF is not the major factor driving the pulmonary tissue changes observed.

Migration of the inflammatory cells into the alveolar space during asthma occurs due to the loosening of the epithelial junctions in the bronchi after damage and shedding of the ciliated cells in the epithelium[6]. Thus, a lower cell number in the lung tissue could be an indication of looser junctions in the epithelium and, therefore, more tissue damage. To investigate this hypothesis, cell infiltration in digested lung tissue was analyzed (Figure 17).

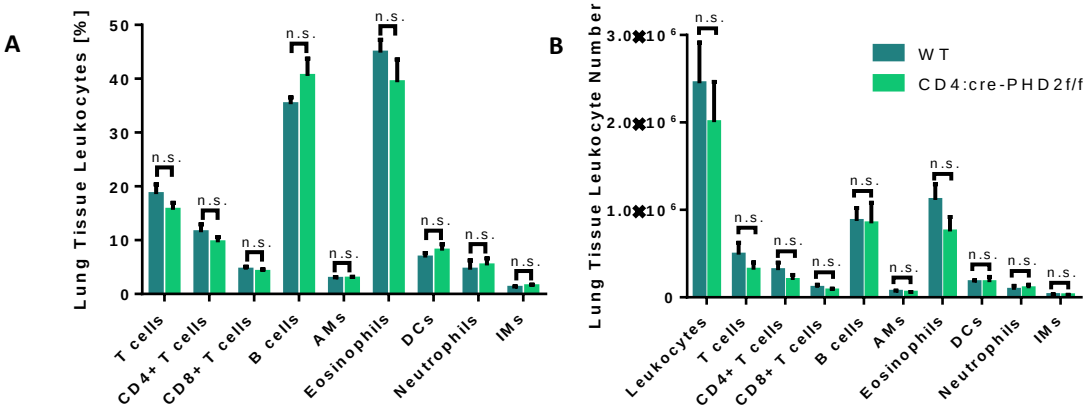

Figure 17 Inflammatory cell infiltration in the lung tissue in CD4:cre-PHD2$^{f/f}$ in the 5 week OVA-induced asthma model. The percentage (A) or total counts (B) of each leukocyte cell population were assessed by flow cytometry in the digested lung tissue of WT-triggered (n=4) and CD4:cre-PHD2$^{f/f}$-triggered mice (n=4). Data are presented as mean ± SEM. n.s. – not significant.

No differences were observed between genotypes in cell percentages in the lung tissue (Figure 17A). There seemed to be a trend for a lower leukocyte number in the lung tissue in the CD4:cre-PHD2$^{f/f}$ mice, however not significant (Figure 17B). This tendency resulted from a high variability between individuals of the same group. Although the same quantity of lung tissue was taken for digestion in order to standardize the cell numbers in the tissue and allow a comparison between groups, this technique has limitations, such as the aforementioned blood contamination, human factors associated with the cutting of the tissue and loss of cells during the filtration process which might explain the obtained results.

However, considering the lack of differences between the groups for either leukocyte amounts in the BALF or in the lung tissue, both genotypes might display similar epithelial barrier damage and at the analyzed time point cell infiltration might not be contributing to the observed phenotype. Therefore, the increased mucus production observed in the CD4:cre-PHD2$^{f/f}$ mice could occur due to higher cell activation and not increased cell numbers in the lung.

2.1.3. Lymph node lymphocyte analysis

As CD4:cre-PHD2$^{f/f}$ mice have a conditional deletion of PHD2 in the T cell compartment and T cell activation by the DCs plays a major role in asthma, the brachial lymph nodes from asthmatic mice were collected and analyzed for each T cell population in regards to their activation state (Figure 18).

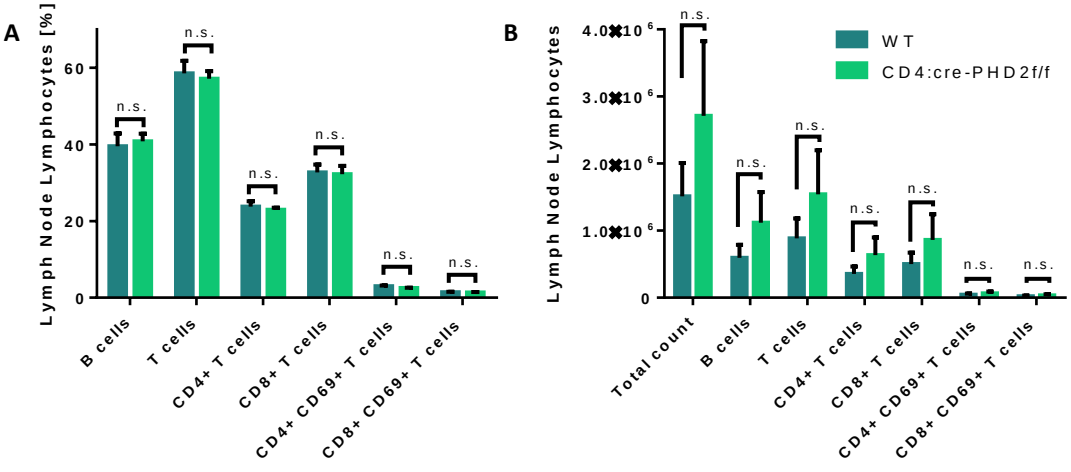

Figure 18 Lymphocyte populations in the lymph node in CD4:cre-PHD2$^{f/f}$ in the 5 week OVA-induced asthma model. The percentage (A) or total counts (B) of each leukocyte cell population were assessed by flow cytometry in the brachial lymph nodes of WT-triggered (n=4) and CD4:cre-PHD2$^{f/f}$-triggered mice (n=4). Data are presented as mean ± SEM. n.s. – not significant.

Analyzing both genotypes with regard to their cell percentages gave no differences between WT and CD4:cre-PHD2$^{f/f}$ mice (Figure 18A). Lymphocyte cell numbers were also comparable between genotypes, although a trend for higher cellularity in the CD4:cre-PHD2$^{f/f}$ mice seemed to exist due to the high variability between individuals in the same group (Figure 18B). Once again the processing of the tissue might have led to a high variable yield that could be interfering with the obtained results.

As the same number of recently activated (CD69^{+}) CD4^{+} T cells existed for both genotypes, it is possible to conclude that the observed phenotype in the CD4:cre-PHD2$^{f/f}$ group is probably independent of the maturation and activation of these cells by the DCs in the lymph nodes. As the T cell numbers in this tissue were also comparable to what was observed in the WT mice, proliferation of the T cells in the lymph nodes is also not enhanced in the cKO.

2.1.4. Whole blood analysis

No differences in leukocyte numbers were observed in BALF, lung or lymph nodes of both genotypes. As this can indicate that at the analyzed time point cell activation and infiltration in the tissue is not occurring at the same extent as it would in the beginning of the asthmatic response, the blood parameters and inflammatory cells in migration were investigated for both genotypes. Blood from asthmatic mice from both groups was analyzed for inflammatory cell levels in order to assess if more cells are in circulation upon asthma triggering. Hematological parameters such as platelets, hemoglobin, hematocrit and white and red blood cells in circulation were the same for both groups (Figure 19), showing that deletion of PHD2 in the T lymphocytes has no effect on these blood elements during asthma induction. Blood analysis was performed using the Sysmex hematological analyzer, which allowed the measurement of each hematological parameter and cell population levels in the blood.

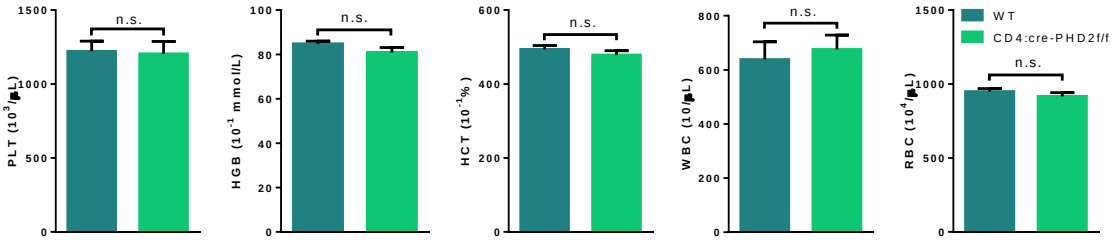

Figure 19 Whole blood quantification of platelets (PLT), hemoglobin (HGB), hematocrit (HCT), white blood cells (WBC) and red blood cells (RBC) in both WT-triggered (n=9) and CD4:cre-PHD2$^{f/f}$-triggered mice (n=10). Measurement of these parameters was performed using a Sysmex hematological analyzer (XT-4000). Data are presented as mean ± SEM. n.s. – not significant.

Comparing the WT asthmatic mice with the CD4:cre-PHD2$^{f/f}$, no discrepancy was observed for the amount of circulating lymphocytes, monocytes, eosinophils or neutrophils (Figure 20).

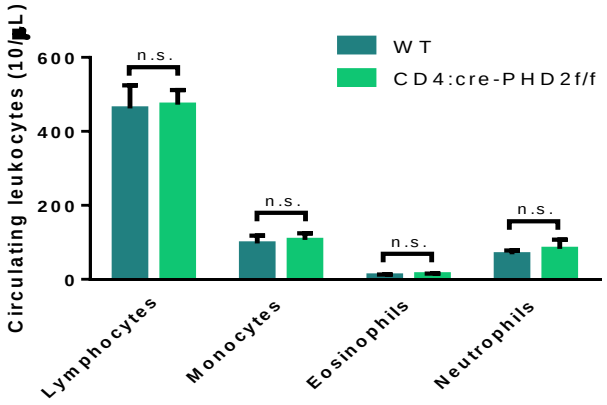

Figure 20 Leukocyte population numbers in circulation in CD4:cre-PHD2$^{f/f}$ in the 5 week OVA-induced asthma model. Leukocyte subpopulations were quantified in both WT-triggered (n=9) and CD4:cre-PHD2$^{f/f}$-triggered mice (n=10) using a Sysmex hematological analyzer (XT-4000). Data are presented as mean ± SEM. n.s. – not significant.

The comparable numbers of the aforementioned leukocytes in circulation indicates that the recruitment of these cells to the tissue is neither impaired nor enhanced in the CD4:cre-PHD2$^{f/f}$ mice, which is in agreement with the cell numbers in both lung tissue and BALF. Although no differences exist between cell numbers in either the BALF or lung tissue in WT or CD4:cre-PHD2$^{f/f}$ mice and the migration of these cells to the tissue is not altered, T cell differentiation might be affected in the cKO mice due to the lack of PHD2 in the T cell compartment.

2.1.5. Th cell differentiation analysis

In order to study the Th cell subpopulations in the lung tissue of asthmatic mice, an intracellular staining was performed for Th2 cells, which are the major cells involved in the eosinophil chemotaxis and activation as well as the induction of the tissue remodeling. Treg cells, on the other hand, have a regulatory effect and are involved in controlling and diminishing the activation of the effector cells[26]. For both WT and CD4:cre-PHD2$^{f/f}$ mice it was possible to observe a cell population positive for both GATA3, the master transcription factor for Th2 cells, and FoxP3, the transcription factor regulating Treg cells (Figure 21). These cells might represent a transient population differentiating from Th2 to Treg, which might indicate the beginning of the resolution of inflammation.

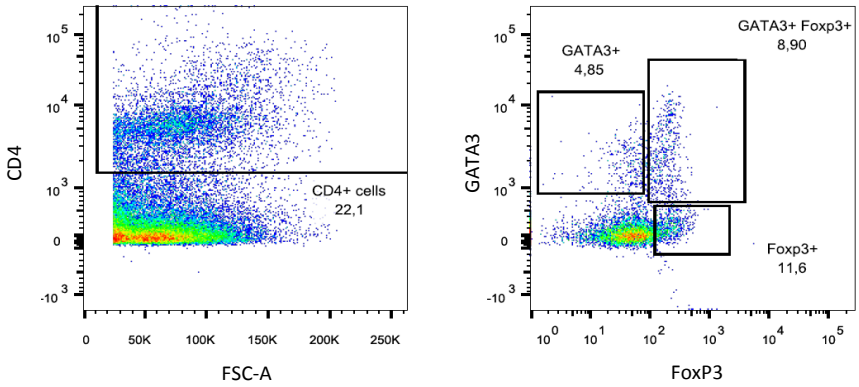

Figure 21 Th cell differentiation in the lung tissue in the 5 week OVA-induced model. Flow cytometry was used to analyze the Th2 (GATA3^{+}) and Treg (FoxP3^{+}) populations in the lung tissue. A population expressing both transcription factors is observed for all samples.

Although GATA3 and FoxP3 were thought to be mutually exclusive transcription factors, Th2 cells have been shown to be able to switch to a Treg phenotype[51]. The double positive (DP) population has been observed in mouse models of allergic asthma by other groups to express both master transcription factors of Treg and Th2 cells, with lower intracellular expression of IL-4, IL-5 and IL-13 comparing to the Th2 cells[51,52]. These Th2 memory-derived Tregs could also actively suppress proliferation and production of cytokines by the Th2 cells, as well as tissue eosinophilia and IgE levels, albeit in a slightly reduced potency when compared to Tregs[51]. Little is known about the mechanisms involved in the aforementioned transition, but it might be induced as a defense response that propitiates the beginning of an anti-inflammatory response in the tissue.

Interestingly, the Th2 fraction was significantly reduced in the CD4:cre-PHD2$^{f/f}$ lungs, whereas Treg cells were induced (Figure 22).

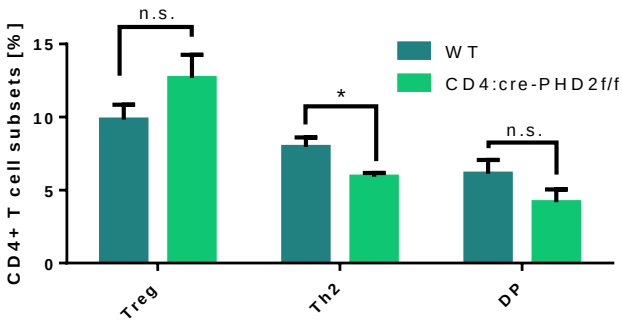

Figure 22 Th cell subpopulations in the lung tissue in CD4:cre-PHD2$^{f/f}$ in the 5 week OVA-induced asthma model. Quantification of the percentage of Th2, Treg and DP cells was done for both WT-triggered (n=3) and CD4:cre-PHD2$^{f/f}$-triggered mice (n=5). Data are presented as mean ± SEM. n.s. – not significant; *p<0.05.

As CD4:cre-PHD2$^{f/f}$ mice show a more severe mucus production, associated with a more intense asthma phenotype, a higher amount of differentiated Th2 cells would be expected, as this Th cell subpopulation is the major intervenient in asthma. However, the existence of a transition population between the Th2 and Treg subsets might indicate that at this stage of disease there is a feedback mechanism that prompts a conversion of the Th2 cells into a regulatory phenotype and therefore no further stimulation of the asthmatic response occurs. The observed Treg population is composed of both nTregs and iTregs generated in the lung tissue. Therefore, the trend for higher Treg percentages in the CD4:cre-PHD2$^{f/f}$ mice might come from increase of iTregs. The cells that originate from this activation suppress the pulmonary DC activation in a more effective manner than the DP population through the production of anti-inflammatory cytokines such as IL-10 and TGF-β[29].

As iTreg cells are generated under the control of DCs with low expression of MHC II[4], quantification of its expression was performed. Mean fluorescence intensity (MFI) due to MHC II staining was measured for the DCs from each analyzed sample (Figure 23), giving the median expression level of MHC II molecules at the surface of each individual cell. Comparing the two genotypes, no difference in MHC II expression was observed on the DCs.

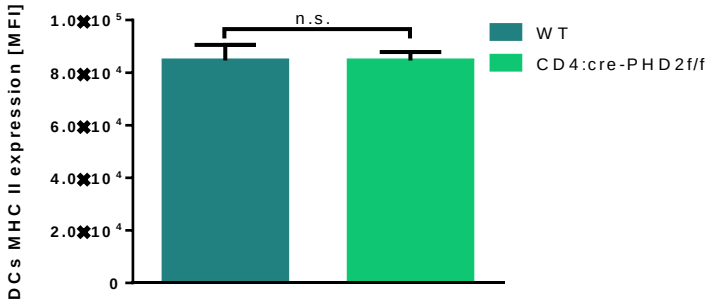

Figure 23 Median expression level of MHC II at the surface of DCs in CD4:cre-PHD2$^{f/f}$ in the 5 week OVA-induced asthma model. Mean fluorescence intensity of the MHC II molecules at the DCs surface was quantified via flow cytometry for both WT-triggered (n=4) and CD4:cre-PHD2$^{f/f}$-triggered mice (n=5). Data are presented as mean ± SEM. n.s. – not significant.

Although a similar expression of this molecule at the surface of the DCs exists between genotypes, other environmental factors such as cytokine levels in the tissue affect iTreg development. The TGF-β signaling is important for the development, survival and function of these cells, but also IL-2 and RA lead to the expansion of iTregs[30]. This last factor is produced by a particular subset of DCs expressing CD103[29] and therefore the expression of this molecule at the surface of the antigen-presenting DCs could be analyzed in the future in order to confirm that no differences exist between genotypes in the Ag presentation that leads to iTregs.

2.1.6. Lung cytokine concentration measurement

Since $CD4^+$ T cell differentiation showed already a transition in the direction of resolution of the inflammatory response, the inflammatory milieu in the tissue originated by a previous inflammatory stimulation could be the major factor driving the observed changes in the epithelial cells in the lung.

As the cytokines produced by the Th2 cells, such as IL-4, IL-5 and IL-13 have an important role in the recruitment of inflammatory cells and in the remodeling observed in the asthmatic tissue[6], their concentration was measured in the homogenates from lung tissue (Figure 24).

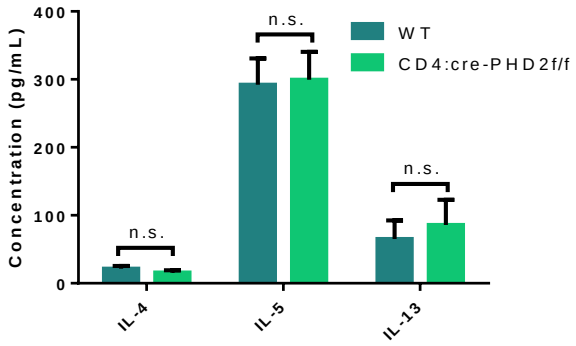

Figure 24 Pro-allergic cytokine concentration in the lung in CD4:cre-PHD2$^{f/f}$ in the 5 week OVA-induced asthma model. IL-4, IL-5 and IL-13 were quantified in the lung tissue of WT-triggered (n=6-8) or CD4:cre-PHD2$^{f/f}$ mice (n=6-10) via ELISA and ECL assays. Data are presented as mean ± SEM. n.s. – not significant.

No differences were found between WT and CD4:cre-PHD2$^{f/f}$ mice. A possible explanation for the lack of difference between the phentotypes might come from the fact that these cells have been triggered for over a week, which might be too long. Shorter time periods of eliciting (e.g. 2-3 days) will therefore have to clarify the discrepancy between the observed increased mucus production and the comparable pro-allergic milieu observed.

During asthma, macrophages are differentiated simultaneously into a M2 phenotype as well as a M1 subtype[36,37]. While the first secrete anti-inflammatory cytokines that potentiate the Th2 differentiation and eosinophil recruitment as well as lung fibrosis, such as IL-13 and TGF-β[37]; M1 cells secrete pro-inflammatory cytokines such as IL-1β, IL-6 and TNF-α, which promote activation of fibroblasts in the tissue, leading to the AHR observed in asthma[36].

IL-1β modulates the constriction of the airway SMC directly and promotes the activation of fibroblasts, being its production by M1 macrophages associated with a higher hyperresponsiveness in the lung with consequent airflow limitation[53].

IL-6 is mainly produced by macrophages, being also released by DCs, B cells and epithelial cells. When produced by APCs, this cytokine induces the initial IL-4 production by the

Th2 cells[55], whereas its production by epithelial cells is associated with an increased stress state of these cells and increased mucus secretion[56].

TNF-α is secreted by several cells, including macrophages, T cells, epithelial cells and SMC. AMs from asthmatic individuals produce higher concentrations of this mediator under IgE stimulation. This cytokine is found in increased amounts in BALF of asthmatic individuals and acts directly on the smooth muscle, increasing its contractibility and contributing to the observed AHR in the patients[36]. TNF-α can also activate eosinophils and macrophages, inducing the production of IL-1β, IL-6 and TNF-α-itself by the latter[57].

As pro-inflammatory cytokines have a role in the pathogenesis of the disease, their levels were quantified via ECL in both WT and CD4:cre-PHD2$^{f/f}$ tissue homogenate. IL-10 was also measured, as this anti-inflammatory cytokine produced mainly by M2 macrophages and Treg cells inhibits the inflammation in the tissue, prompting the resolution of the asthmatic response[36] (Figure 25).

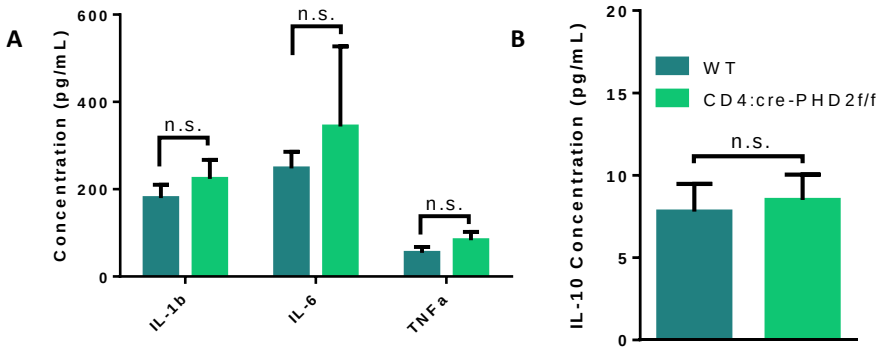

Figure 25 Pro- and anti-inflammatory cytokine concentration in the lung in CD4:cre-PHD2$^{f/f}$ in the 5 week OVA-induced asthma model. Pro-inflammatory cytokines IL-1β, IL-6 and TNF-α (A) as well as anti-inflammatory cytokine IL-10 (B) were quantified in the lung tissue of WT-triggered (n=6) or CD4:cre-PHD2$^{f/f}$ mice (n=6) via ECL assays. Data are presented as mean ± SEM. n.s. – not significant.

Although a slight tendency was observed for higher concentration of pro-inflammatory cytokines in the homogenized lung tissue from the CD4:cre-PHD2$^{f/f}$ mice, no significant differences in IL-1β, IL-6 or TNF-α levels were observed between genotypes (Figure 25A).

The lack of a clear increase in the IL-1β concentration in the CD4:cre-PHD2$^{f/f}$ mice is in accordance with the absence of differences between genotypes in collagen deposition surrounding the bronchi. The comparable concentration between genotypes of TNF-α also correlates with the lack of differences in the levels of the remainder pro-inflammatory cytokines analyzed.

As for IL-6 levels, the slight increase in its concentration observed in the CD4:cre-PHD2$^{f/f}$ mice, could be due to the higher production of this cytokine by the epithelium and not

by the macrophages in the tissue, since the mucus secretion in the bronchi is elevated comparing with the WT.

Regarding the IL-10 concentration, both genotypes express the same level of this cytokine in the lung homogenate (Figure 25B), which is not in agreement with the trend for higher Treg percentage in the CD4:cre-PHD2$^{f/f}$ mice. However, Treg cells represent only a fraction of the IL-10-producing cells in the tissue and the increased production of this cytokine by these cells might be insignificant when measuring IL-10 in tissue homogenate.

The similarity in cytokine concentration between genotypes might be associated with the observed transition to a resolution of inflammation in the tissue and, therefore, measurement of these mediators at this phase is not elucidatory of the mechanism that drives the higher susceptibility of the CD4:cre-PHD2$^{f/f}$ mice to asthma. Differences in the cytokine production that ultimately leads to the tissue remodeling in the lung might exist at an earlier phase of the response, creating a need for measurement of these mediators in previous time points.

2.1.7. Serum IgE concentration measurement

Under normal conditions, IgE exists in minute amounts in circulation. However, during an allergic response, Th2 cells induce the Ig class switching of the antibodies produced by the B cells into IgE via IL-4 production, leading to the increase of this antibody levels in the blood[31]. This antibody is specific for the antigen used in the triggering of the asthmatic response and has long-lived interactions with inflammatory cells such as eosinophils, inducing the production of leukotrienes by these cells and therefore contributing for the bronchoconstriction in the lung tissue[33]. IgE concentration was measured in the serum of the analyzed mice using ELISA (Figure 26).

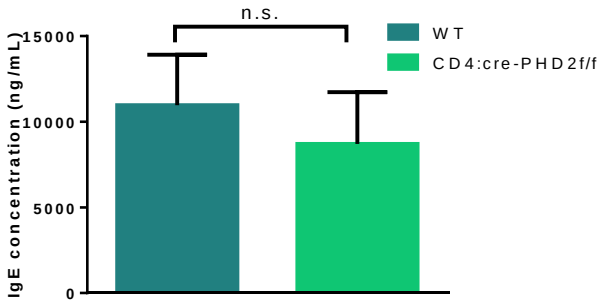

Figure 26 IgE levels in the serum of CD4:cre-PHD2$^{f/f}$ mice in the 5 week OVA-induced asthma model. IgE concentration was measured in the serum of WT-triggered (n=10) and CD4:cre-PHD2$^{f/f}$ mice (n=10). Data are presented as mean ± SEM. n.s. – not significant.

No differences were observed between genotypes. As IgE stimulation of the AMs in the lung leads to the increased production of IL-1β, IL-6 and TNF-α[33] the comparable concentration of IgE in both WT and CD4:cre-PHD2$^{f/f}$ mice corroborates the lack of difference in concentration of these cytokines in the lung tissue. As IgE has a very short half-life in circulation, of less than a day[31], the measured similar concentration between genotypes might be the result of the analogous concentration of IL-4 at the time of analysis.

Asthma is characterized by an early-phase response which involves the activation and infiltration of inflammatory cells in the lung tissue and a late-phase response, which is associated with tissue remodeling that leads to the increased mucus production, AHR and bronchoconstriction observed in the patients. The aforementioned comparable levels of cells, cytokines and mediators between the WT and CD4:cre-PHD2$^{f/f}$ mice might indicate that at the analyzed time point these factors have reached a plateau and that the differences in mucus production are the outcome of distinct concentrations of these mediators at an earlier time point. Therefore, all of the analyzed parameters suggest the reaching of a late-phase response in the asthmatic mice.

The 5 week OVA model allowed the characterization of a more extreme asthmatic phenotype regarding the Goblet cell metaplasia in the CD4:cre-PHD2$^{f/f}$ mice, which is associated with a trend for higher vascular remodeling that hinders the perfusion of the tissue. Although no differences in cell infiltration and cytokine concentration were observed between the two groups, a tendency for increased conversion of the pro-allergic response into an resolution phase exists for the CD4:cre-PHD2$^{f/f}$ mice. This might, thus, be indicative of a late-phase during the disease and at which point several hallmarks of the disease are severely expressed. Unfortunately, this avoids the correct characterization of the mechanism through which the differences between genotypes occur. Therefore, a milder model of the disease could contribute to the unraveling of the mechanism that modulates the more severe phenotype in the CD4 cKO.

2.2. 2 week OVA-induced Asthma Model

As the asthma phenotype aggravated in the CD4:cre-PHD2$^{f/f}$ mice compared to WT littermates, with extensive vascular remodeling that limits the perfusion of the lung tissue, a shorter model was used in order to assess if the difference was also maintained in a milder model of airway allergy.

2.2.1. Tissue remodeling evaluation

Histological analysis was performed to study Goblet cell coverage in the bronchi and vascular remodeling in this model, as these were the two major hallmarks altered in the CD4:cre-PHD2$^{f/f}$ in the 5 week OVA model (Figures 27 and 28).

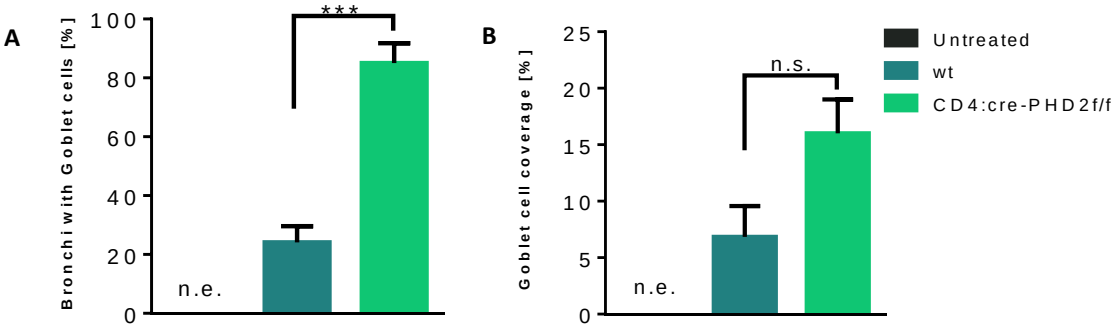

Figure 27 Goblet cell quantification in lung sections from untreated WT (n=2), WT-triggered (n=5) and CD4:cre-PHD2$^{f/f}$-triggered mice (n=5) in the 2 week OVA-triggered asthma model. The percentage of bronchi expressing Goblet cells (A) and the overall Goblet cell coverage in the lung (B) were measured. Data are presented as mean ± SEM. n.e. – not expressed; n.s. – not significant; ***p<0.001.

Treatment with OVA in the 2 week model leads to an increase in the percentage of bronchi expressing Goblet cells (Figure 27A). This increase is significantly higher in the CD4:cre-PHD2$^{f/f}$ mice, following a similar trend to what was obtained in the 5 week model. However, the Goblet cell coverage in the lung shows no significant differences after triggering, although there is a trend for increased coverage in the CD4:cre-PHD2$^{f/f}$ genotype (Figure 27B). This tendency resembles the increased Goblet cell coverage observed in the 5 week model and might indicate that this model could be used as an alternative to the aforementioned 5 week OVA-induced asthma.

Regarding the vascular remodeling in the lung tissue after asthmatic triggering, no differences between untreated and treated mice were observed (Figure 28).

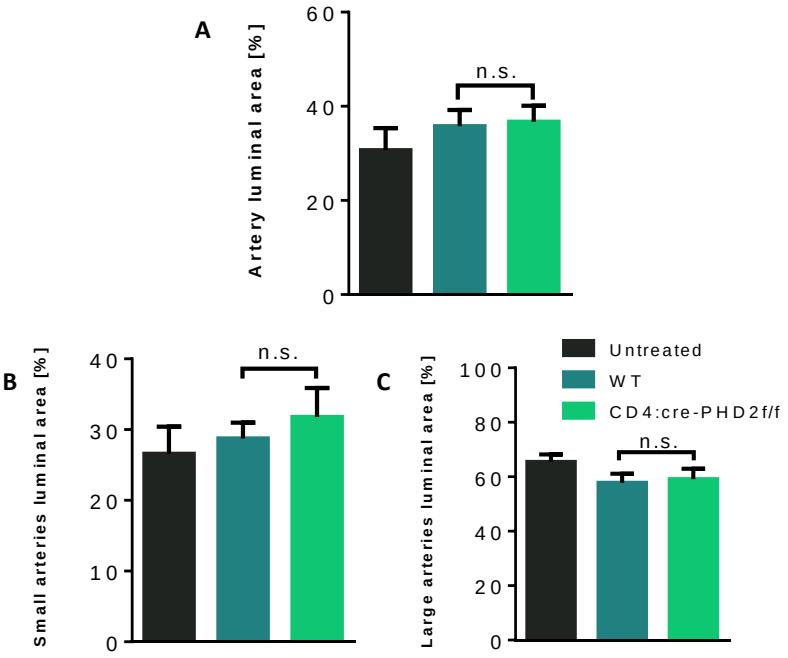

Figure 28 Quantification of the vascular remodeling in the lung in CD4:cre-PHD2$^{f/f}$ in the 2 week OVA-induced asthma model. Lung sections from untreated WT (n=2), WT-triggered (n=5) and CD4:cre-PHD2$^{f/f}$-triggered (n=5) were analyzed using ImageJ. Vascular luminal area is expressed as the ratio between the lumen area of the vessel and the total area of the vessel. Small vessels depict vessels with a total area smaller than 10mm^2, being the large vessels of sizes above the aforementioned. Data are presented as mean ± SEM. n.s. – not significant.

The milder phenotype observed, with no changes in vascular thickening, allowed the successful perfusion of the lung tissue of both WT and CD4:cre-PHD2$^{f/f}$ mice affected with airway allergy.

As the tissue remodeling observed in the 2 week OVA-induced asthma follows a similar trend to what was observed in the 5 week model with regard to the mucus production, this model could be representative of a similar, but milder, response as to what obtained in the previous model analyzed. The lack of vascular remodeling allows the perfusion of the lung tissue, contributing to a better removal of the blood from the tissue and allowing more reliable inflammatory cell quantification in the lung.

2.2.2. Inflammatory cell infiltration analysis

Cell infiltration in the BALF was assessed with flow cytometry in order to study which are the main cell populations in this asthma model that might characterize the phenotype (Figure 29).

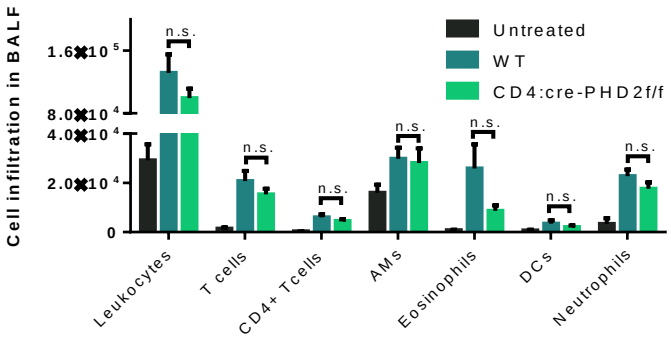

Figure 29 Inflammatory cell infltration in the BALF in CD4:cre-PHD2$^{f/f}$ in the 2 week OVA-induced asthma model. The total counts of each leukocyte cell population were assessed by flow cytometry in the BALF of untreated WT (n=3), WT-triggered (n=9) and CD4:cre-PHD2$^{f/f}$-triggered mice (n=9). Data are presented as mean ± SEM. n.s. – not significant.

Upon asthmatic triggering, leukocyte infiltration was observed in the BALF, of mainly T cells, particularly CD4^{+}, and neutrophils in the same extent in both genotypes. No significant eosinophilia was observed in this model, indicating that the major cells involved in the observed tissue remodeling are not the same as in the 5 week model. Infiltration of neutrophils into the BALF is not representative of the majority of asthma conditions, which are characterized by a high eosinophilia[23].

The 2 week OVA-induced asthma model elicits a similar, albeit milder Goblet cell coverage to what is obtained with the 5 week OVA-induced asthma model. Interestingly, the observed trend pointed to a more severe phenotype in the CD4:cre-PHD2$^{f/f}$ mice in regards of this parameter. This milder triggering also has the advantage of not leading to the vascular remodeling that represented a hindrance in perfusion of the lung tissue. However, major infiltrating cells in this model of the disease are not the eosinophils, but also the neutrophils. This outcome is distinct from what occurs in the 5 week OVA-induced model and does not resemble the majority of asthma cases, as only a minority of the asthmatic patients has neutrophilia associated with their condition[23]. As this model might not be representative for the regular asthmatic phenotype, another short-term airway allergy model was established in order to assess the response in both genotypes under conventional asthma.

2.3. HDM-induced Asthma Model

OVA-induced asthma models are widely accepted in the study of this disease, but these require a sensitization period in order to elicit the allergy, as mice are not naturally allergic to this protein. HDM, however, is a common allergen in humans and induces an allergic response in mice without the need of previous sensitization[50]. As HDM models involve less triggering events than the OVA model, they resemble a more natural airway allergy. The asthma phenotype was assessed in WT and CD4:cre-PHD2$^{f/f}$ using this allergen.

2.3.1. Tissue remodeling evaluation

As histological analysis is the most reliable way to assess the asthmatic phenotype, PAS staining was performed in sections from both genotypes (Figure 30).

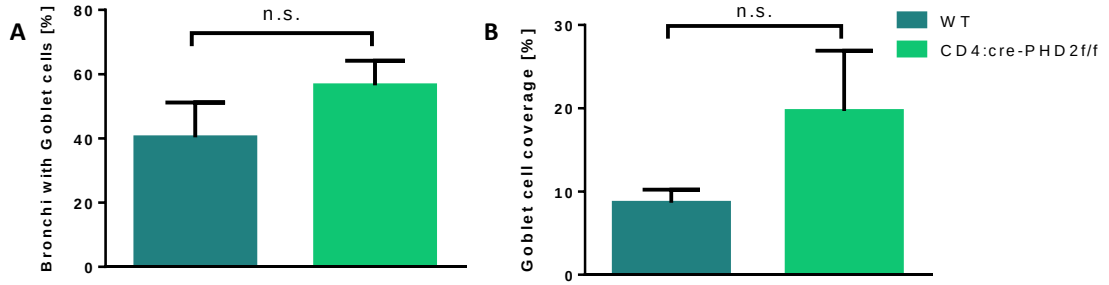

Figure 30 Goblet cell quantification in lung sections from WT-triggered (n=2) and CD4:cre-PHD2$^{f/f}$-triggered mice (n=4) in the HDM-induced asthma model. The percentage of bronchi expressing Goblet cells (A) and the overall Goblet cell coverage in the lung (B) were measured. Data are presented as mean ± SEM. n.s. – not significant.

Although not significant, there is a trend for higher Goblet cell coverage in the CD4:cre-PHD2$^{f/f}$ mice comparing with the WT mice treated with HDM. However, the analyzed groups are very small (n=2 for the WT, n=4 for the cKO), being only indicative of a possible phenotypic difference between the CD4:cre-PHD2$^{f/f}$ mice and the WT littermates, but not allowing to conclude that indeed a higher airway remodeling exists. This could, however, indicate that the observed phenotype in the 5 week OVA model is reproducible in the HDM model and that this should be further explored to assess other hallmarks of the disease. Further experiments will be required to confirm this hypothesis.

2.3.2. Inflammatory cell Infiltration analysis

After induction of the airway allergy with the HDM, there was an influx of leukocytes into the BALF, with an influx of mainly eosinophils and T cells (Figure 31).

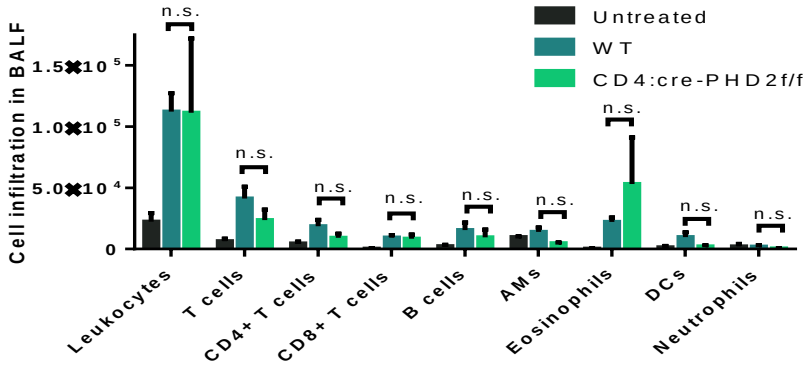

Figure 31 Inflammatory cell infltration in the BALF in CD4:cre-PHD2$^{f/f}$ in the HDM-induced asthma model. The total quantification of each leukocyte cell population was assessed by flow cytometry in the BALF of untreated WT (n=2), WT-triggered (n=5) and CD4:cre-PHD2$^{f/f}$-triggered mice (n=4). Data are presented as mean ± SEM. n.s. – not significant.

Comparing both groups, identical cell infiltration in the BALF was observed. This outcome is in agreement to what observed in the 5 week OVA-induced model and confirms that cell infiltration in the BALF is not altered in the CD4:cre-PHD2$^{f/f}$ mice.

2.3.3. Serum IgE concentration measurement

Assessing IgE levels in the serum, no differences were obtained between genotypes (Figure 32).

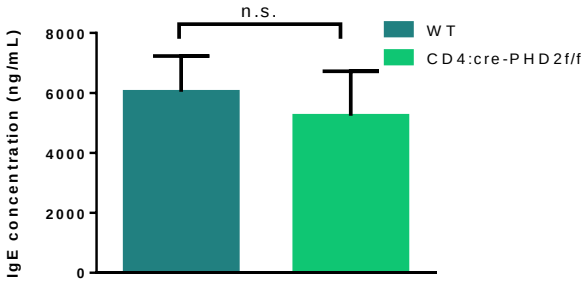

Figure 32 IgE levels in the serum of CD4:cre-PHD2$^{f/f}$ mice in the HDM-induced asthma model. IgE concentration was measured in the serum of WT-triggered (n=5) and CD4:cre-PHD2$^{f/f}$ mice (n=4). Data are presented as mean ± SEM. n.s. – not significant.

As IgE production by the B cells is induced by the IL-4 secreted by the activated Th2 cells upon antigen presentation by the DCs[31], the observed similar concentration of this antibody in circulation might be an indicator of a comparable IL-4 concentration at the time of

analysis and of a similar phenotype to that observed in the 5 week OVA asthma model. Further analysis of cytokine levels in the tissue, as well as Th cell differentiation should be performed to confirm this hypothesis.

Albeit the fact that in either studied asthma models no differences in cell infiltration and in several mediators are observed, there is a trend for a harsher phenotype in the CD4:cre-PHD2$^{f/f}$ asthmatic mice for both a 5 week OVA-induced asthma model and an HDM-induced asthma model. This outcome is indicative of a higher susceptibility for airway allergy in the CD4:cre-PHD2$^{f/f}$ mice, suggesting that PHD2 might have a protective role in the T cells during asthma.

3. The Role of PHD2 and PHD3 in Myeloid cells during Asthma

All three PHD family members can hydroxylate and consequently inactivate HIFα. However, PHD2 has been described as the major HIF prolyl hydroxylase, as its inactivation with specific small interfering RNA (siRNA) is sufficient for the robust induction of HIFα in spite of the presence of PHD1 and PHD3[17]. Nevertheless, deletion of either PHD1 or PHD3 in conjunction with PHD2 leads to the modulation of the HIF response in distinct manners, having a compensatory effect upon hypoxia conditions in the protection against continued lack of oxygen. PHD3 was described as a HIF1α target, being its transcription markedly induced under hypoxic conditions. This protein has a very potent role in the negative regulation of HIF2α[15]. Therefore, PHD3 represents a link between HIF1α and HIF2α, maintaining a tight balance between the activation of these two transcription factors[20], and being involved in a feedback loop to suppress HIF activation under prolonged hypoxia[19].

As the mice with deletion of PHD2 in the myeloid compartment did not shown a higher susceptibility to the airway allergy in a 5 week OVA-induced model, a possible protective role of HIF1α through the upregulation of PHD3 and consequent inhibition of HIF2α in these cells was considered. To assess the role of the ensuing PHD3 activation in these cells, LysM:cre-PHD2$^{f/f}$ PHD3$^{f/f}$ were submitted to a 5 week OVA model of airway allergy.

3.1. Inflammatory cell Infiltration Analysis

Cell infiltration in the BALF of both WT and LysM:cre-PHD2$^{f/f}$ PHD3$^{f/f}$ triggered mice was analyzed through flow cytometry. As one of the three performed experiments elicited a higher cell infiltration in all mice, which could be due to other environmental factors at the time of the experiment, cell infiltration is represented as a relative amount in comparison with the average of each individual WT groups (Figure 33).

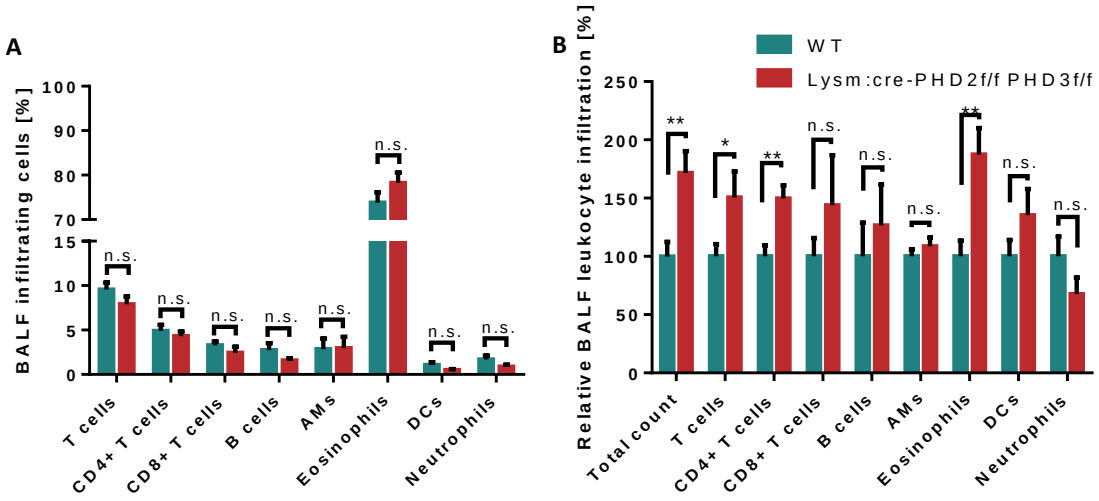

Figure 33 Inflammatory cell infiltration in the BALF of LysM:cre-PHD2$^{f/f}$ PHD3$^{f/f}$ mice in the 5 week OVA-induced asthma model. The percentage (A) or relative counts (B) of each leukocyte cell population were assessed by flow cytometry in the BALF of WT-triggered (n=11) and LysM:cre-PHD2$^{f/f}$ PHD3$^{f/f}$-triggered mice (n=8). In (B) the average of each WT group in each individual experiment was set to 100%, being the cell numbers in the cKO represented in relation to this value. Data are presented as mean ± SEM. n.s. – not significant; *p<0.05; **p<0.01.

Interestingly, contrary to what was observed in the CD4:cre-PHD2$^{f/f}$ mice, the LysM:cre-PHD2$^{f/f}$ PHD3$^{f/f}$ mice showed a higher cell infiltration in the BALF comparing to the OVA-triggered WT. This difference was mainly due to higher CD4^{+} T cell and eosinophil numbers in this fluid. The increased number of these cells was observed in every individual experiment and could indicate a more severe asthma phenotype in these mice, as CD4^{+}T cells and eosinophils modulate the majority of downstream effects observed in this disease[6].

To assess if a higher severity of the asthmatic phenotype is present in these mice, parameters such as cytokine production, IgE in circulation and tissue remodeling were analyzed.

3.2. Lung Cytokine Concentration Measurement

Comparing Th2 cytokine levels in the analyzed mice, no differences were observed (Figure 34).

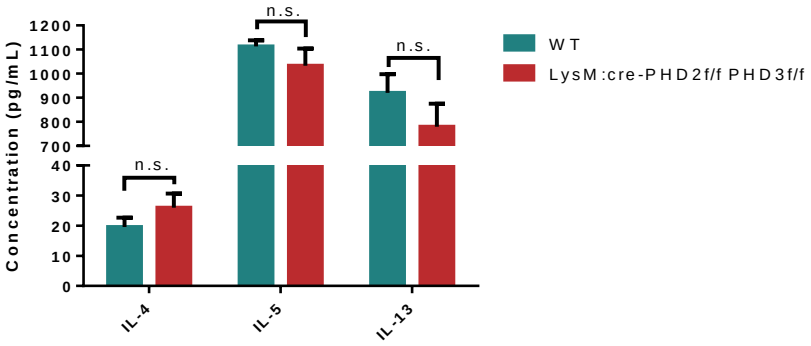

Figure 34 Pro-allergic cytokine concentration in the lung in the LysM:cre-PHD2$^{f/f}$ PHD3$^{f/f}$ mice. IL-4, IL-5 and IL-13 were quantified in the lung tissue of WT-triggered (n=6) or LysM:cre-PHD2$^{f/f}$ PHD3$^{f/f}$ mice (n=6) via ELISA and ECL assays. Data are presented as mean ± SEM. n.s. – not significant.

LysM:cre-PHD2$^{f/f}$ PHD3$^{f/f}$ mice showed increased cell infiltration in the BALF, mainly of CD4^{+} T cells and eosinophils. The latter are attracted to the lung by the production of eotaxin by the Th2 cells[25] and therefore a higher pro-allergic cytokine concentration was expected. The observed similarity in cytokine production could indicate that, at the analyzed time point, production of these cytokines by the Th2 cells has yet to occur. Therefore, after four days of triggering cells might be still at a point of initial migration into the tissue.

Analyzing the pro-inflammatory cytokines in the tissue, there was a trend for reduced levels in the LysM:cre-PHD2$^{f/f}$ PHD3$^{f/f}$ mice compared to WT littermates (Figure 35A). Although these cytokines contribute to the airway remodeling in the tissue, they inhibit the differentiation of T cells into the Th2 subset and might therefore be detrimental to the recruitment and activation of this subset.

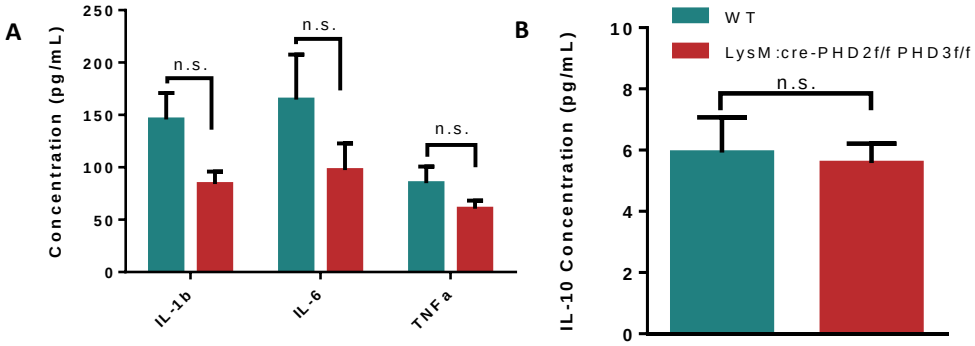

Figure 35 Pro- and anti-inflammatory cytokine concentration in the lung of LysM:cre-PHD2$^{f/f}$ PHD3$^{f/f}$ mice. Pro-inflammatory cytokines IL-1β, IL-6 and TNF-α (A) as well as anti-inflammatory cytokine IL-10 (B) were quantified in the lung tissue of WT-triggered (n=6) or LysM:cre-PHD2$^{f/f}$ PHD3$^{f/f}$ mice (n=6) via ECL assays. Data are presented as mean ± SEM. n.s. – not significant.

The lower concentration of pro-inflammatory cytokines could be indicative of lower differentiation of the macrophages into a M1 phenotype due to a higher M2 differentiation by these cells and, therefore, the establishment of an environment more prone to Th2 differentiation. As modulation of PHD2 and PHD3 in these mice is done at a myeloid cell level, affecting some cells at the first line of defense in the tissue, it might be that in these mice the asthmatic response is still in an early phase at the analyzed time point. Measurement of TGF-β levels in these mice could give further insight regarding the differentiation of the macrophages in the LysM:cre-PHD2$^{f/f}$ PHD3$^{f/f}$ mice. Regarding the IL-10 concentration (Figure 35B), no differences between the groups were observed. If the asthmatic response in these mice is still at an early phase during the point of analysis, the production of this cytokine might still be inhibited by the inflammatory cells that are present in the tissue, which could explain the comparable observed concentration between genotypes.

3.3. Serum IgE Concentration Measurement

A slight trend for higher concentration of IgE in circulation was observed for the LysM:cre-PHD2$^{f/f}$ PHD3$^{f/f}$ mice, albeit not significant (Figure 36).

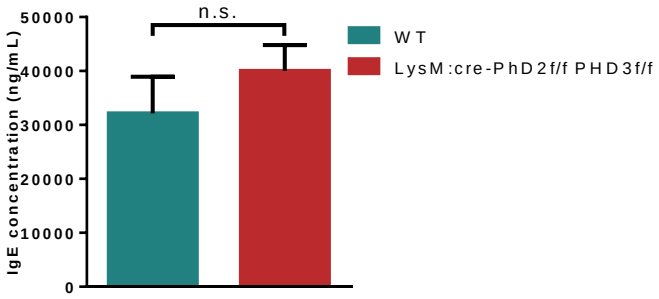

Figure 36 IgE levels in the serum of LysM:cre-PHD2$^{f/f}$ PHD3$^{f/f}$ asthmatic mice in the 5 week OVA-induced asthma model. IgE concentration was measured in the serum of WT-triggered (n=6) and LysM:cre-PHD2$^{f/f}$ PHD3$^{f/f}$ mice (n=6). Data are presented as mean ± SEM. n.s. – not significant.

IgE is produced under stimulation of the B cells by the activated Th2 cells and induces the further generation of this CD4^{+}T cell subset in the lymph nodes when bound to the surface of DCs[31]. This antibody also stimulates leukotriene production by the eosinophils in the lung[33], and its mild increase in the LysM:cre-PHD2$^{f/f}$ PHD3$^{f/f}$ might be consistent with a higher eosinophil activity in the lung and, therefore, of a harsher phenotype of the disease.

3.4. Tissue Remodeling Evaluation

To assess the tissue remodeling in these mice after asthmatic triggering, Goblet cell coverage was analyzed for both OVA-treated WT and LysM:cre-PHD2$^{f/f}$ PHD3$^{f/f}$ (Figure 37).

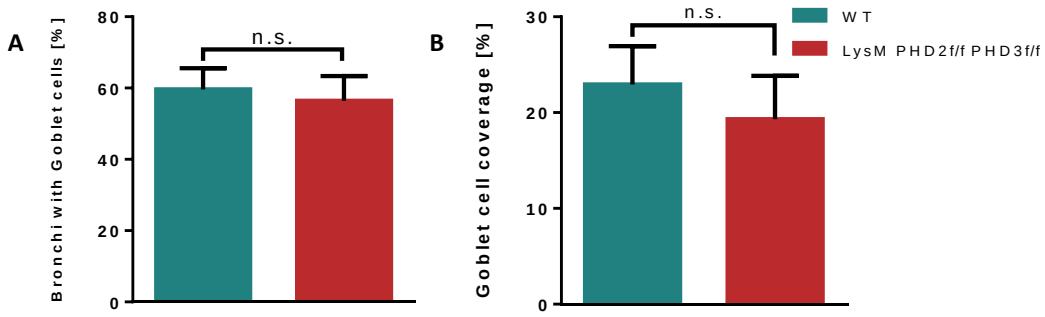

Figure 37 Goblet cell quantification in lung sections from WT-triggered (n=6) and LysM:cre-PHD2$^{f/f}$ PHD3$^{f/f}$-triggered mice (n=6). The percentage of bronchi expressing Goblet cells (A) and the overall Goblet cell coverage in the lung (B) were measured. Data are presented as mean ± SEM. n.s. – not significant.

Although the cell infiltration in the BALF and proinflammatory cytokine levels in the lung tissue seem to be in agreement with an induction of the Th2 differentiation and, therefore, a harsher asthma phenotype in the LysM: cre PHD2$^{f/f}$ PHD3$^{f/f}$, the Goblet cell occupation in the bronchi is comparable to what observed in the WT asthmatic mice. Neither the percentage of Goblet cell-expressing bronchi (Figure 33A) nor the overall coverage of these cells (Figure 33B) was altered in the cKO mice.

As the modulation of PHD2 and PHD3 in these mice occurs in the myeloid compartment, affecting macrophages, myeloid-derived DCs and possibly eosinophils and neutrophils, the changes caused by the deletion of these proteins might interfere with an initial step in asthma. Therefore, the analyzed time point might represent an initial stage of the disease in this genotype. Additional triggering and later analysis of these mice should be done to further describe the asthmatic response and overall phenotype in these mice.

Nevertheless, the higher infiltration of CD4^{+} T cells and eosinophils in the BALF of the LysM:cre-PHD2$^{f/f}$ PHD3$^{f/f}$ mice suggests that the migration of these cells to the area of damage is enhanced and might contribute for a more severe phenotype which might not be reflected in the remodeling of the tissue. Future work needs to be done to assess if HIF1α activation in the myeloid cells has a protective role through the activation of PHD3 and consequent inhibition of HIF2α.

Conclusions and Future Work

The hypoxic environment established upon asthmatic triggering contributes to the increased cell infiltration and tissue damage observed in asthmatic patients, leading to dyspnea, AHR and sputum production. Although systemic inhibition of the hypoxia pathway has been shown to reduce the disease outcome[7,21], little is known about the role of this pathway in the inflammatory cells involved in the development of asthma.

The study of the role of oxygen sensors in inflammatory diseases is currently widespread and well established, allowing the modulation of these proteins in individual cell types. As T cells and myeloid cells have a significant role in the pathogenesis of asthma, modulating the hypoxia response in these cells might shed light on the particular aspects of this pathway in these cells.

In a model of OVA-induced lung inflammation, PHD2-deficiency in the T cell compartment of mice (CD4:cre-PHD2$^{f/f}$) leads to a higher mucus production by the epithelial cells in the bronchus. This higher secretion seems to be mediated by metaplasia but not hyperplasia of the epithelial cells into Goblet cells. Although no differences between genotypes are apparent in collagen deposition surrounding the bronchi, the higher mucus production by the CD4:cre-PHD2$^{f/f}$ bronchi, as well as higher vascular remodeling in the lung is an indicator of a more severe asthmatic phenotype. This mucus production phenotype is observed for the 5 week OVA-induced asthma model as well as the HDM-induced asthma model. This strongly suggests that there is indeed a higher susceptibility of the CD4:cre-PHD2$^{f/f}$ mice to the asthmatic condition.

Lung tissue remodeling is the outcome of an inflammatory milieu and of the signaling of pro-allergic and pro-inflammatory cytokines. The lack of difference in the levels of these mediators between mice lacking PHD2 in the T cells and their WT littermates is counter-intuitive considering the overall outcome of the disease. However, this might arise from the fact that in both genotypes the concentration of this cytokines might plateau after four days of asthmatic triggering. Indeed, CD4^{+} T cells at this time point show a conversion from a Th2 phenotype, majorly involved in the pathogenesis of asthma, to a Treg phenotype that suppresses the inflammatory response and might represent the initiation of the resolution of inflammation[51,52].

To unravel the mechanism that leads to the observed higher sensitivity in the CD4:cre-PHD2$^{f/f}$ mice, future studies need to focus on the analysis of a time point preceding the one analyzed in this work. Cell infiltration, as well as IgE in circulation and cytokine levels in the

tissue should be assessed, as these factors are the major contributors to the early-phase response that occurs in asthma. qPCR or ELISAs on cell pellet from fluorescence-activated sorted cells will contribute to the identification of the cells involved in the production of the mediators that contribute to the disease outcome. $CD4^+$ T cell differentiation during this period needs also to be studied, as this mechanism seems to be altered at a later time point. *In vitro* recall assays will be performed to facilitate the study of the potential differentiation of these cells under stimulation of the antigen. The combination of all these approaches will allow a further understanding of the protective role of PHD2 in the T cells during asthma.

A mouse strain lacking PHD2 and PHD3 in the T cell compartment (CD4:cre-$PHD2^{f/f}$ $PHD3^{f/f}$) is currently being established. As deletion of both oxygen sensors in the myeloid compartment (LysM:cre-$PHD2^{f/f}PHD3^{f/f}$) reveals an expansion of the sensitivity window, with delayed inflammatory response in the lung tissue upon asthma triggering, the induction of airway allergy in CD4:cre-$PHD2^{f/f}$ $PHD3^{f/f}$ might elicit a similar outcome. Future studies will therefore focus on the analysis of the feedback mechanism between PHD2 and PHD3 in the T cell compartment and its influence in the asthmatic outcome.

PHD3 is involved in a feedback loop to suppress HIF, particularly HIF2α, under prolonged hypoxia. The induction of the transcription of this protein during HIF1α induction might have a protective role during asthma. Indeed, the results obtained in this work demonstrate that deletion of both PHD2 and PHD3 in the myeloid compartment contributes to a higher cell infiltration in the BALF during asthma, with a marked influx of $CD4^+$ T cells and eosinophils, the major intervenient cells in this disease. Albeit the higher cell influx, no increase in mucus production could be revealed in the LysM:cre-$PHD2^{f/f}$ $PHD3^{f/f}$ mice versus their WT littermates. This, associated with the trend for reduced pro-inflammatory cytokine levels in the lung tissue, might suggest that the mice were evaluated during the initial phase of the disease, indicated by the infiltration of the cells in the lung and establishment of a propitious environment for the differentiation of $CD4^+$ T cells into a Th2 phenotype.

Future studies need to assess this question by measuring cell infiltration, tissue remodeling and cytokine concentration in the lung tissue at later time points, as four days of triggering might be insufficient to observe the effect of the PHD2 and PHD3 deletion in the myeloid cells in the pathology of asthma. As the modulation of the aforementioned PHDs occurs in the monocytes, macrophages, as well as myeloid-derived DCs, the activation and recruitment of T cells might be altered in these mice. *In vitro* co-culture of allergen-pulsed DCs from LysM:cre-$PHD2^{f/f}$ $PHD3^{f/f}$ mice with WT T cells or adaptive transfer of these cells into naïve mice might help elucidate the mechanisms involved in this recruitment. Also, similar

studies need to be performed to analyze the capacity of the pulmonary macrophages to inhibit the DCs activation and migration to the lymph nodes.

Overall, this work has described for the first time a protective role of PHD2 in the T cells during asthma, indicating also a possible role for PHD3 in the myeloid compartment in the control of this disease. Further study of the mechanism of both models might contribute to the development of novel therapies and therefore a better management of a yet to be controlled disease.

References

1. Bousquet, J., Clark, T. J., Hurd, S., Khaltaev, N., Lenfant, C., O'Byrne, P. (2007). "GINA guidelines on asthma and beyond". Allergy, 62(2):102–112.
2. Tattersfield, A.E., Knox, A.J., Britton, J.R., Hall, I.P. (2002). "Asthma", The Lancet, 360: 1313-1322.
3. Martinez, F.D., Vercelli, D. (2013). "Asthma", The Lancet, 382:1360-1372.
4. Cohn, L., Elias, J.A., Chupp, G.L. (2004). "Asthma: Mechanisms of Disease Persistence and Progression", Annual Review of Immunology, 22:789-815.
5. Fahy, J.V. (2015). "Type 2 inflammation in asthma — present in most, absent in many", Nature Reviews Immunology 15:57–65.
6. Kudo, M., Ishigatsubo, Y., Aoki, I. (2013). "Pathology of asthma", Frontiers in Microbiology, 4.
7. Ahmad, T., Kumar, M., Mabalirajan, U., Pattnaik, B., Aggarwal, S., Singh, R., Singh, S., Mukerji, M., Ghosh, B., Agrawal, A. (2012). "Hypoxia response in asthma: differential modulation on inflammation and epithelial injury". American Journal of Respiratory Cell and Molecular Biology, 47(1):1-10.
8. Huerta-Yepez, S., Baay-Guzman, G.J., Bebenek, I.G., Hernandez-Pando, R., Vega, M.I., Chi, L., Riedl, M., Diaz-Sanchez, D., Kleerup, E., Tashkin, D.P., Gonzalez, F.J., Bonavida, B., Zeidler, M., Hankinson, O. (2011). "HIF promotes murine allergic airway inflammation and is increased in asthma and rhinitis", Allergy, 66(7):909–918.
9. Eltzschig, H.K., Bratton, D.K., Colgan, S.P. (2014). "Targeting hypoxia signalling for the treatment of ischaemic and inflammatory diseases", Nature Reviews Drug Discovery, 13:852-869.
10. Mamlouk, S., Kalucka, J., Pal Singh, R., Franke, K., Muschter, A., Langer, A., Jakob, C., Gassmann, M., Baretton, G., Wielockx, B. (2013). "Loss of prolyl hydroxylase-2 in myeloid cells and T-lymphocytes impairs tumor development". International Journal of Cancer, 134(4):849-858.
11. Wang, G.L., Jiang, B-H., Rue, E.A., Semenza, G.L. (1995). "Hypoxia-inducible factor 1 is a basic-helix-loop-helix-PAS heterodimer regulated by cellular O2 tension", Proceedings of the National Academy of Sciences USA, 92:5510–5514.
12. Rabinowitz, M. (2013). "Inhibition of Hypoxia-Inducible Factor Prolyl Hydroxylase Domain Oxygen Sensors: Tricking the Body into Mounting Orchestrated Survival and Repair Responses". Journal of Medical Chemistry, 56 (23):9369–9402.
13. Jaakkola, P., Mole, D., Tian, Y., Wilson, M., Gielbert, J., Gaskell, S., von Kriegsheim, A., Hebestreit, H., Mukherji, M., Schofield, C., Maxwell, P., Pugh, C., Ratcliffe, P. (2001). "Targeting of HIF-alpha to the von Hippel-Lindau ubiquitylation complex by O2-regulated prolyl hydroxylation". Science, 292(5516):468-72.
14. Déry, M., Michaud, M., Richard, D. (2005). "Hypoxia-inducible factor 1: regulation by hypoxic and non-hypoxic activators". The International Journal of Biochemistry & Cell Biology, 37:535-540.

15. Appelhoff, R., Tian, Y., Raval, R., Turley, H., Harris, A., Pugh, C., Ratcliffe, P., Gleadle, J. (2004). "Differential function of the prolyl hydroxylases PHD1, PHD2, and PHD3 in the regulation of hypoxia-inducible factor". The Journal of Biological Chemistry, 279(37):38458-38465.
16. Palazon, A., Goldrath, A., Nizet, V., Johnson, R. (2014). "HIF Transcription Factors, Inflammation and Immunity". Immunity, 41(4):518–528.
17. Berra, E., Benizri, E., Ginouves, A., Volmat, V., Roux, D., Pouyssegur, J. (2003). "HIF prolyl-hydroxylase 2 is the key oxygen sensor setting low steady-state levels of HIF-1alpha in normoxia". EMBO Journal, 22(16): 4082-4090.
18. Minamishima, Y., Moslehi, Y., Bardeesy, N., Cullen, D., Bronson, R., Kaelin, W. (2008). "Somatic inactivation of the PHD2 prolyl hydroxylase causes polycythemia and congestive heart failure". Blood, 111:3236–3244.
19. Minamishima, Y., Moslehi, J., Padera, R., Bronson, R., Liao, R., Kaelin, W. (2009). "A feedback loop involving the Phd3 prolyl hydroxylase tunes the mammalian hypoxic response in vivo". Molecular and Cellular Biology, 29(21):5729-5741.
20. Franke, K., Kalucka, J., Mamlouk, S., Singh, R., Muschter, A., Weidemann, A., Iyengar, V., Jahn, S., Wieczorek, K., Geiger, K., Muders, M., Sykes, A., Poitz, D., Ripich, T., Otto, T., Bergmann, S., Breier, G., Baretton, G., Fong, G., Greaves, D., Bornstein, S., Chavakis, T., Fandrey, J., Gassmann, M., Wielockx, B. (2013). "HIF-1α is a protective factor in conditional PHD2-deficient mice suffering from severe HIF-2α-induced excessive erythropoiesis". Blood, 121(8):1436-1445.
21. Huerta-Yepez, S., Baay-Guzman, G.J., Garcia-Zepeda, R., Hernandez-Pando, R., Vega, M.I., Gonzalez-Bonilla, C. (2008). "2-Methoxyestradiol (2-ME) reduces the airway inflammation and remodeling in an experimental mouse model". Clinical Immunology, 129:313–324.
22. Toussaint, M., Fievez, L., Drion, P., Cataldo, D., Bureau, F., Lekeux, P., Desmet, C. (2013). "Myeloid hypoxia-inducible factor 1α prevents airway allergy in mice through macrophage-mediated immunoregulation". Mucosal Immunology, 6(3):485-497.
23. Wenzel, S. (2013). "Complex phenotypes in asthma: Current definitions". Pulmonary Pharmacology & Therapeutics, 26:710-715.
24. Lambrecht, B., Hammad, H. (2003). "Taking our breath away: dendritic cells in the pathogenesis of asthma". Nature Reviews Immunology, 3:994-1003.
25. Corrigan, C., Kay, A. (1992). "T cells and eosinophils in the pathogenesis of asthma". Immunology Today, 13(12):501-507.
26. Lloyd, C.M., Hessel, E.M. (2010). "Functions of T cells in asthma: more than just TH2 cells". Nature Reviews Immunology, 10(12):838-848.
27. Lindén, A., Laan, M., Anderson, G. (2005). "Neutrophils, interleukin-17A and lung disease". European Respiratory Journal, 25:159–172.
28. Lee, H., Bautista, J., Hsieh, C. (2011). "Thymic and peripheral differentiation of regulatory T cells". Advances in Immunology, 112:25-71.

29. Dons, E., Raimondi, G., Cooper, D., Thomson, A. (2012). “Induced regulatory T cells: mechanisms of conversion and suppressive potential”. Human Immunology, 73(4):328-334.
30. Belkaid, Y., Oldenhove, G. (2008). “Tuning microenvironments: Induction of regulatory T cells by dendritic cells”. Immunity, 29:362–371.
31. Platts-Mills, T. (2001). "The Role of Immunoglobulin E in Allergy and Asthma", American Journal of Respiratory and Critical Care Medicine, 164(8): S1-S5.
32. Yssel, H., Abbal, C., Pène, J., Bousquet, J. (1998). “The role of IgE in asthma”. Clinical & Experimental Allergy, 28: 104–109.
33. Gould, H., Sutton, B. (2008). “IgE in allergy and asthma today”. Nature Reviews Immunology, 8(3):205-217.
34. Balhara, J., Gounni, A. (2012). “The alveolar macrophages in asthma: a double-edged sword”. Mucosal Immunology, 5(6):605-609.
35. Peters-Golden, M. (2004). "The Alveolar Macrophage". American Journal of Respiratory Cell and Molecular Biology, 31(1): 3-7.
36. Moreira, A., Hogaboam, C. (2011). “Macrophages in allergic asthma: fine-tuning their pro- and anti-inflammatory actions for disease resolution.” Journal of Interferon & Cytokine Research, 31(6):485-491.
37. Pappas, K., Papaioannou, A., Kostikas, K., Tzanakis, N. (2013). “The role of macrophages in obstructive airways disease: chronic obstructive pulmonary disease and asthma”. Cytokine, 64(3):613-25.
38. Gleich, G.J. (2000). “Mechanisms of eosinophil-associated inflammation”. Journal of Allergy and Clinical Immunology, 105:651-663.
39. Rothenberg, M., Hogan, S. (2006). “The Eosinophil”. Annual Reviews Immunology, 24:147–174.
40. Nair, P., Pizzichini, M., Kjarsgaard, M., Inman, M., Efthimiadis, A., Pizzichini, E. (2009). “Mepolizumab for prednisone-dependent asthma with sputum eosinophilia”. The New England Journal of Medicine, 360:985–993.
41. Deckers, J., Madeira, F., Hammad, H. (2013). “Innate immune cells in asthma”. Trends in Immunology, 34(11):540-547.
42. Kawakami, T., Kashiwakura, J., Kawakami, Y. (2014). “Histamine-Releasing Factor and Immunoglobulins in Asthma and Allergy”. Allergy, Asthma and Immunology Research, 6(1):6-12.
43. Ciepiela, O., Ostafin, M., Demkow, U. (2015). “Neutrophils in asthma—A review”. Respiratory Physiology & Neurobiology, 209:13-16.
44. Pak, O., Aldashev, A., Welsh, D., Peacock, A. (2007). “The effects of hypoxia on the cells of the pulmonary vasculature”. European Respiratory Journal, 30:364–372.
45. Rydell-Törmänen, K., Risse, P., Kanabar, V., Bagchi, R., Czubryt, M., Johnson, J. (2013). “Smooth muscle in tissue remodeling and hyper-reactivity: Airways and arteries”. Pulmonary Pharmacology & Therapeutics, 26:13-23.

46. Meyer-Martin, H., Reuter, S., Taube, C. (2014). “T-Helper Cells - Mouse Models of Allergic Airway Disease”. Methods in Molecular Biology, 1193:127-141.
47. Gueders, M., Paulissen, G., Crahay, C., Quesada-Calvo, F., Hacha, J., Van Hove, C., Tournoy, K., Louis, R., Foidart, J., Noël, A., Cataldo, D. (2009). “Mouse models of asthma: a comparison between C57BL/6 and BALB/c strains regarding bronchial responsiveness, inflammation, and cytokine production”. Inflammation Research, 58(12):845-854.
48. Pae, S., Cho, J., Dayan, S., Miller, M., Pemberton, A., Broide, D. (2010). “Chronic allergen challenge induces bronchial mast cell accumulation in BALB/c but not C57BL/6 mice and is independent of IL-9”. Immunogenetics, 62(8):499-506.
49. Nials, A. T., Uddin, S. (2008). “Mouse models of allergic asthma: acute and chronic allergen challenge”. Disease Models & Mechanisms, 1(4-5): 213–220.
50. Vivek D. Gandhi, V., Davidson, C., Asaduzzaman, M., Nahirney, D., Vliagoftis, H. (2013). “House Dust Mite Interactions with Airway Epithelium: Role in Allergic Airway Inflammation”. Current Allergy and Asthma Reports, 13(3):262-270.
51. Kima, B., Kima, I., Parka, Y., Kima, Y., Kima, Y., Changa, W., Leea, Y., Kweonb, M., Chungc, Y., Kanga,C. (2009). “Conversion of Th2 memory cells into Foxp3+ regulatory T cells suppressing Th2-mediated allergic asthma”. Proceedings of the National Academy of Sciences, 107(19): 8742–8747.
52. Reubsaet, L., Meerding, J., Giezeman, R., Kleer, I., Arets, B., Prakken, B., Beekman, J., Wijk, F. (2013). “Der p 1–induced $CD4^+$ $FOXP3^+$ $GATA3^+$ T cells have suppressive properties and contribute to the polarization of the TH2-associated response”. J. Allergy Clin Immunol, 132(6): 1440-1444.
53. Hakonarson, H., Herrick, D., Serrano, P., Grunstein, M. (1997). “Autocrine role of interleukin 1beta in altered responsiveness of atopic asthmatic sensitised airway smooth muscle”. Journal of Clinical Investigation, 99: 117–124.
54. Krause, K., Metz, M., Makris, M., Zuberbier, T., Maurer, M. (2012). „The role of interleukin-1 in allergy-related disorders”. Current Opinion in Allergy and Clinical Immunology, 12(5):477-484.
55. Doganci, A., Sauer, K., Karwot, R., Finotto, S. (2005). “Pathological role of IL-6 in the experimental allergic bronchial asthma in mice”. Clinical Reviews in Allergy & Immunology, 28(3):257-270.
56. Rincon, M., Irvin, C. (2012). “Role of IL-6 in asthma and other inflammatory pulmonary diseases”. International Journal of Biological Sciences, 8(9):1281-1290.
57. Waserman, S., Dolovich, J., Conway, M., Marshall, J. (2000). “TNF-alpha dysregulation in asthma: relationship to ongoing corticosteroidtherapy”. Canadian Respiratory Journal, 7(3):229-37.

Appendix

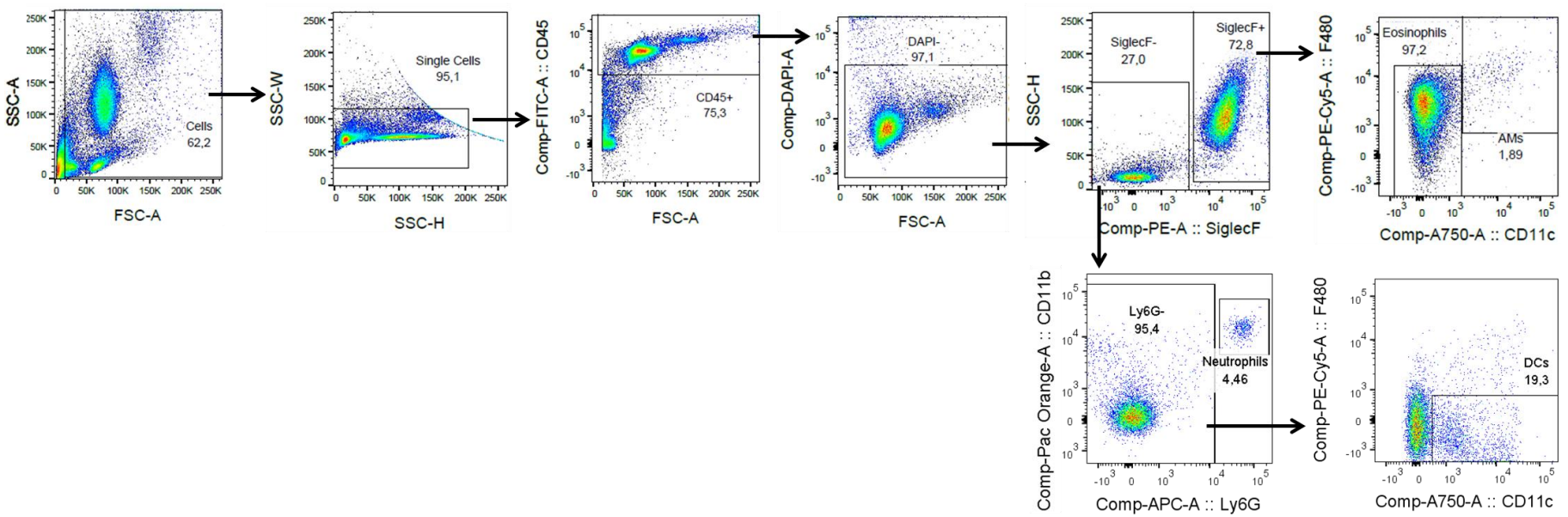

Figure 38 Myeloid staining gating strategy.

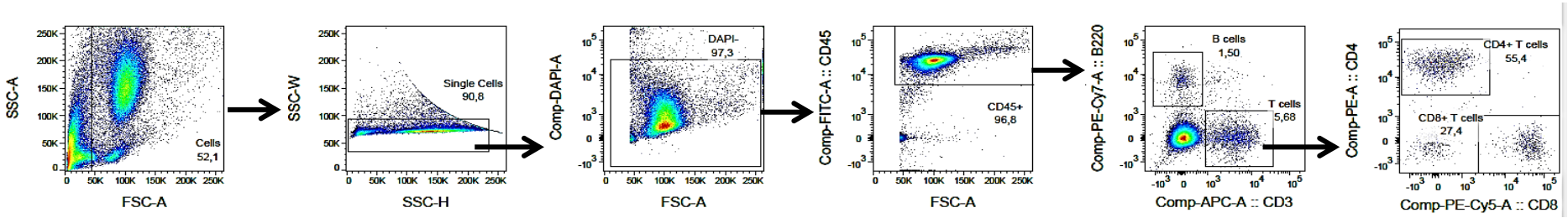

Figure 39 Lymphoid staining gating strategy.

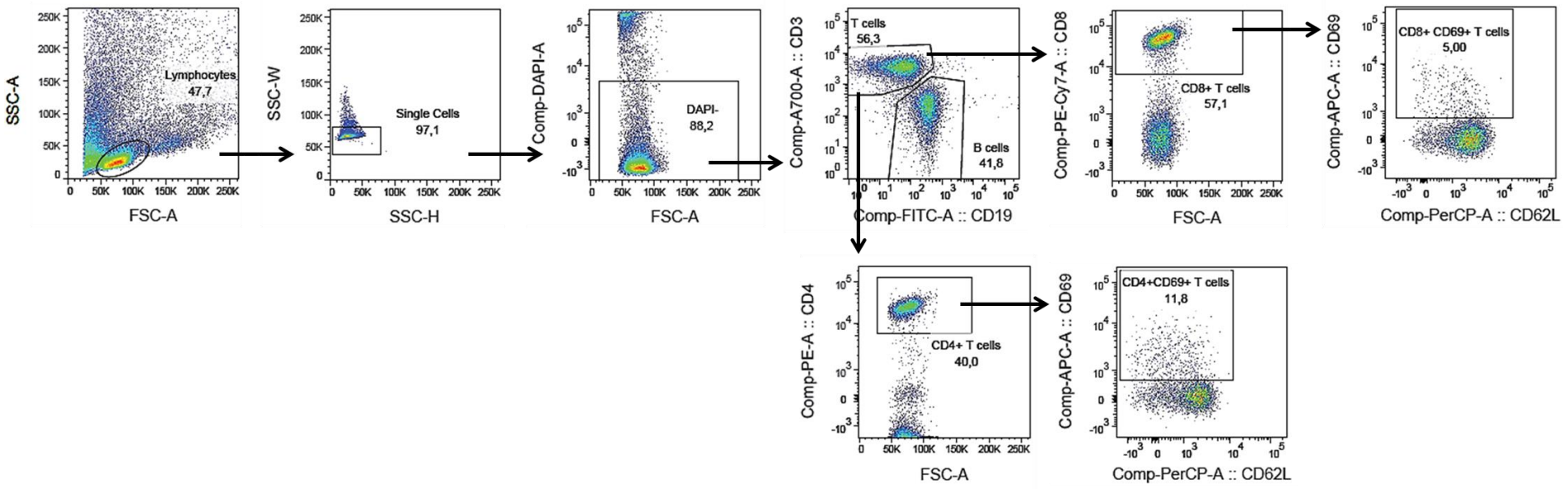

Figure 40 Lymph node staining gating strategy.

b